Extratropical storm inundation testbed: Intermodel comparisons in Scituate, Massachusetts

Changsheng Chen,[1,2] Robert C. Beardsley,[3] Richard A Luettich Jr.,[4] Joannes J. Westerink,[5] Harry Wang,[6] Will Perrie,[7] Qichun Xu,[1] Aaron S. Donahue,[5] Jianhua Qi,[1] Huichan Lin,[1] Liuzhi Zhao,[1] Patrick C. Kerr,[5] Yanqiu Meng,[6] and Bash Toulany[7]

[1] The Integrated Ocean Observing System Super-regional Coastal Modeling Testbed had one objective to evaluate the capabilities of three unstructured-grid fully current-wave coupled ocean models (ADCIRC/SWAN, FVCOM/SWAVE, SELFE/WWM) to simulate extratropical storm-induced inundation in the US northeast coastal region. Scituate Harbor (MA) was chosen as the extratropical storm testbed site, and model simulations were made for the 24–27 May 2005 and 17–20 April 2007 ("Patriot's Day Storm") nor'easters. For the same unstructured mesh, meteorological forcing, and initial/boundary conditions, intermodel comparisons were made for tidal elevation, surface waves, sea surface elevation, coastal inundation, currents, and volume transport. All three models showed similar accuracy in tidal simulation and consistency in dynamic responses to storm winds in experiments conducted without and with wave-current interaction. The three models also showed that wave-current interaction could (1) change the current direction from the along-shelf direction to the onshore direction over the northern shelf, enlarging the onshore water transport and (2) intensify an anticyclonic eddy in the harbor entrance and a cyclonic eddy in the harbor interior, which could increase the water transport toward the northern peninsula and the southern end and thus enhance flooding in those areas. The testbed intermodel comparisons suggest that major differences in the performance of the three models were caused primarily by (1) the inclusion of wave-current interaction, due to the different discrete algorithms used to solve the three wave models and compute water-current interaction, (2) the criterions used for the wet-dry point treatment of the flooding/drying process simulation, and (3) bottom friction parameterizations.

1. Introduction

[2] Coastal inundation along the U.S. East Coast is defined as flooding of dry land caused generally by hurricanes (tropical cyclones) and extratropical cyclones [*Bernier and Thompson*, 2006]. Storms can generate strong winds and high surge, and the combined wind waves and storm surge during high tide can produce significant inundation and severe damage in the coastal zone. In Massachusetts, coastal inundation is frequently caused by strong extratropical cyclones (e.g., nor'easters) and much less frequent tropical cyclones. In the past 30 years, more than 15 notable nor'easters swept through New England, but only two hurricanes were recorded [http://en.wikipedia.org/wiki/Nor%27easter]. For example, the April 2007 extratropical cyclone (the "Patriot's Day Storm") had a center barometric pressure as low as 968 hPa and an intensity similar to a moderate category II hurricane. The storm produced strong winds (peak gusts above 70 m/s) and 8 m waves above high tides (1.2 m above normal) and caused serious coastal flooding in eastern Massachusetts (esp. Cape Ann to Nantucket), with damage of ~$216M in New England [*National Weather Center*, 2007; *McFadden*, 2007].

[3] The NOAA National Weather Service (NWS) has primary responsibility for forecasting coastal hazards including surface winds, waves, storm surge, and

[1]School for Marine Science and Technology, University of Massachusetts-Dartmouth, New Bedford, Massachusetts, USA.

[2]International Center for Marine Studies, Shanghai Ocean University, Shanghai, China.

[3]Department of Physical Oceangraphy, Woods Hole Oceanographic Institution, Woods Hole, Massachusetts, USA.

[4]Institute of Marine Sciences, University of North Carolina, Morehead City, North Carolina, USA.

[5]Department of Civil and Environmental Engineering and Earth Sciences, University of Notre Dame, Notre Dame, Indiana, USA.

[6]Virginia Institute of Marine Science, College of William and Mary, Gloucester Point, Virginia, USA.

[7]Fisheries and Oceans Canada, Bedford Institute of Oceanography, Dartmouth, Nova Scotia, Canada.

Corresponding author: C. Chen, School for Marine Science and Technology, University of Massachusetts-Dartmouth, 706 S. Rodney French Blvd., New Bedford, MA 02744, USA. (c1chen@umassd.edu)
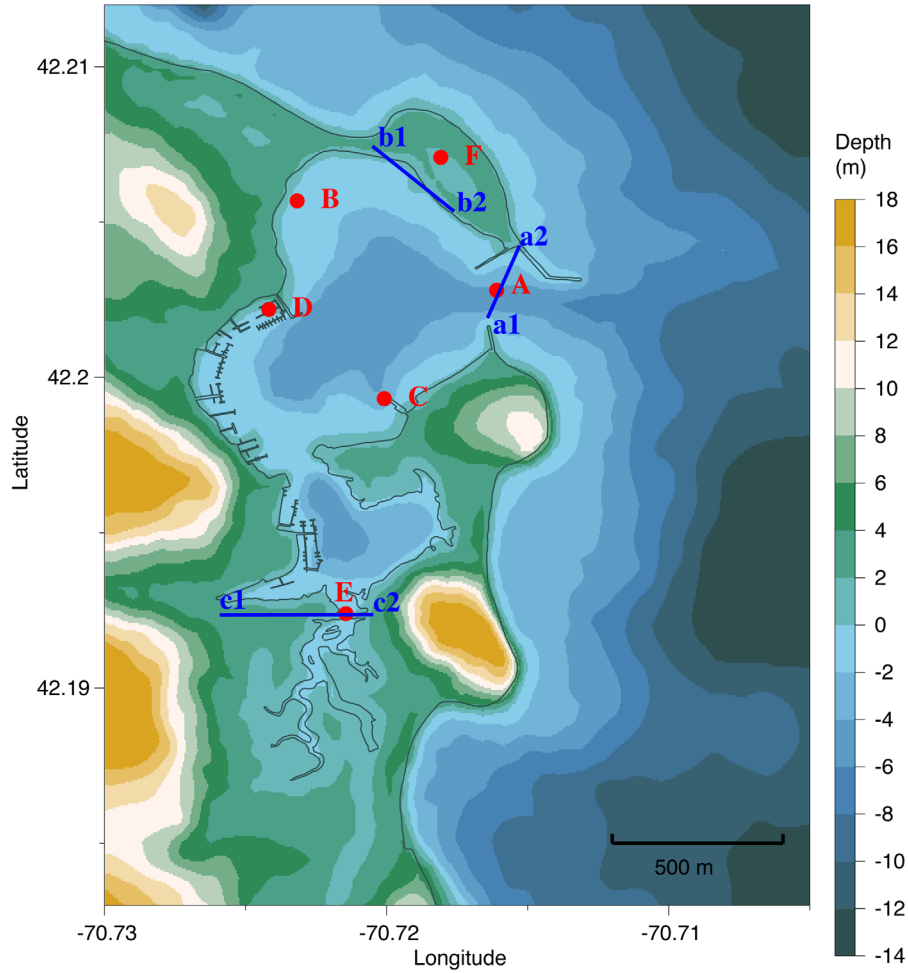
Figure 1. Bathymetry of Scituate Harbor, MA. Colors are the water and land height in meters, with negative values for the water depth and positive values for the land height. Sites labeled A-E (marked by dots) and transects labeled a1-a2, b1-b2, and c1-c2 (marked by blue straight lines) were the places selected for the time series comparison of water elevation, significant wave height, and net volume fluxes among ADCIRC, FVCOM, and SELFE.

inundation. The NWS Weather Forecast Offices (WFOs) in Taunton (MA) and Grey (ME) selected Scituate as its first pilot site to improve its coastal inundation forecast capability. The Northeast Regional Association of Coastal Ocean Observing Systems (NERACOOS) was established in late 2007 as part of the NOAA-led US Integrated Ocean Observing System (IOOS). The modeling component of NERACOOS has two primary objectives: establishing a regional ocean forecast system and developing the capability for "end-to-end" inundation forecasting in Scituate (Figure 1). In the last three years, the University of Massachusetts-Dartmouth (UMassD) and Woods Hole Oceanographic Institution (WHOI) FVCOM development team has made significant progress in establishing the Northeast Coastal Ocean Forecast System (NECOFS) and placing the FVCOM-based Scituate inundation forecast model into operation (http://fvcom.smast.umassd.edu/).

[4] In 2010, NOAA-led IOOS launched a Super-regional Testbed to Improve Models of Environmental Processes for the U.S. Atlantic and Gulf of Mexico coasts program in 2010 (http://testbed.sura.org/). One objective of the inun-

dation/storm surge component was to evaluate the capabilities of three unstructured-grid fully current-wave coupled ocean models (ADCIRC/SWAN, FVCOM/SWAVE, SELFE/WWM) to simulate extratropical storm-induced inundation in the northeast. Scituate was chosen as the extratropical storm testbed site to take advantage of the existing FVCOM-SWAVE inundation forecast model development by NECOFS and desire to use the testbed results to improve NWS WFO inundation warning forecasts. The 24–27 May 2005 and 17–20 April 2007 (Patriot's Day Storm) nor'easters both caused significant flooding and were selected for study.

[5] ADCIRC, FVCOM, and SELFE are fully nonlinear primitive equation unstructured-grid coastal ocean models with the same governing equations and turbulent closure schemes [*Chen et al.*, 2003, 2006a, 2006b, 2011; *Luettich and Westerink*, 2004; *Zhang and Baptista*, 2008]. The difference between these models is mainly in the discrete algorithm used: ADCIRC and SELFE are coded with the finite-element method and FVCOM with the finite-volume method. These models were validated for benchmark test

problems and numerous applications for consistency, stability, convergence, conservation, boundedness, and reality. Conceptually, for given same forcings and parameterizations, the discrete schemes used in these models should all converge toward the same solution, as the model resolution is refined. In real applications, however, due to restrictions of computational resources and efficiency, these models are frequently run with insufficient horizontal resolution to capture the key multiscale processes. Under such conditions, the models may perform differently, not only in numerical accuracy but also in dynamical responses to external forcing.

[6] The surface wave models implemented in these three models are different: SWAN for ADCIRC [*Zijlema*, 2010], SWAVE for FVCOM [*Qi et al.*, 2009], and WWM for SELFE [*Roland*, 2009]. Although the governing equations for these models are the same, discrete algorithms used to solve the wave spectrum density equation and dynamic assumptions made in the current-wave coupling could lead to differences in simulation results and hence coastal inundation. By using the same unstructured mesh and same storm-induced external and boundary forcing, we evaluated these models for their dynamical responses in inundation simulations, particularly on the impact of current-wave interaction on coastal inundation in Scituate.

[7] This paper summarizes the intermodel comparison results of ADCIRC, FVCOM, and SELFE for the 2005 and 2007 extratropical storm simulations. The remaining sections are organized as follows. Section 2 describes the three models and the numerical experiments, including the grid configuration, external forcing, and initial/boundary conditions. Section 3 presents the simulation results for experiments with (a) only tidal forcing and (b) cases without and with inclusion of current-wave interaction. Section 4 discusses the intermodel comparisons with a focus on the three surface wave models. Section 5 summarizes the conclusions.

2. Model Descriptions and Numerical Designs

2.1. Descriptions of ADCIRC, FVCOM, and SELFE

[8] The intermodel comparisons for extratropical storm inundation experiments were made using ADCIRC, FVCOM, and SELFE. These three models utilize unstructured triangular meshes to resolve the complex irregular coastal geometry and wet-dry treatment methods to simulate the coastal inundation process [*Luettich and Westerink*, 2004; *Dietrich et al.*, 2012; *Chen et al.*, 2006b, 2007; *Zhang et al.*, 2011]. ADCIRC and FVCOM were run by the model development teams [ADCIRC—University of Notre Dame (UND); FVCOM—UMassD-WHOI], while SELFE was run by Virginia Institute of Marine Science (VIMS) with technical support from the Oregon Health and Science University. A brief description of these three models is given below.

2.1.1. ADCIRC

[9] ADCIRC is the ADvanced CIRCulation Model developed originally by *Luettich and Westerink* [2004] and upgraded through a team effort with the University of North Carolina (UNC), UND, and collaborators [*Dawson et al.*, 2006; *Dietrich et al.*, 2012]. The ADICRC model used in this study is the two-dimensional (2-D) depth-integrated

version called ADCIRC-2DDI (hereafter referred to as "ADCIRC"), which is a continuous-Galerkin finite-element code that solves the depth-integrated shallow water equations on an unstructured triangular mesh [*Luettich and Westerink*, 2004; *Dawson et al.*, 2006] with parameterization of bottom friction by the Manning formulation. The ADCIRC model has been coupled with the unstructured-mesh version of the Simulating WAves Nearshore (SWAN) model so that both models run on the same unstructured mesh and on the same computational cores [*Zijlema*, 2010; *Dietrich et al.*, 2012]. SWAN is advanced forward in time using a first-order implicit time stepping algorithm [*Zijlema*, 2010]. Coupling is achieved through the transfer of wave radiation stress from SWAN to ADCIRC, and water levels, currents, and frictional roughness lengths from ADCIRC to SWAN. This transfer occurs at intervals of 600 s, which is equivalent to the SWAN time step used for these simulations. The resulting ADCIRC/SWAN model is aimed at simulating accurately and efficiently the propagation of wind waves, tides, and storm surge from deep water into the nearshore. This coupled model has been used in simulating the complex response characteristics of hurricane-induced storm surges in the Northern Gulf of Mexico [*Tanaka et al.*, 2011; *Dietrich et al.*, 2012] and for the design and analysis of the Flood Risk Reduction System for southeastern Louisiana [*USACE*, 2009; *FEMA*, 2009]. The model validation for storm surge simulation was carried out for recent hurricanes including Katrina (2005), Rita (2005), Gustav (2008), and Ike (2008) [*Bunya et al.*, 2010; *Dietrich et al.*, 2010, 2011; *Kennedy et al.*, 2011; *Hope et al.*, 2013].].

2.1.2. FVCOM

[10] FVCOM is the three-dimensional (3-D) primitive equation unstructured grid, general terrain-following coordinate, Finite-Volume Community Ocean Model developed originally by *Chen et al.* [2003] and upgraded by the UMassD-WHOI model development team [*Chen et al.*, 2006a, 2006b, 2007, 2008; *Lai et al.*, 2010a, 2010b; *Huang et al.*, 2008; *Chen et al.*, 2011]. FVCOM utilizes the second-order approximate finite-volume discrete algorithm with an integral form of governing equations over momentum and tracer control volumes in the terrain-following generalized vertical coordinate system with either Cartesian coordinates [*Chen et al.*, 2003] or spherical coordinates [*Chen et al.*, 2006b, 2011], and is integrated with time with options of a mode-split solver in which external and internal modes are advanced in tandem at different time steps [*Chen et al.*, 2003] and a semi-implicit solver with a single time step inversely proportional to water current magnitude [*Chen et al.*, 2009; *Chen et al.*, 2011; *Lai et al.*, 2010a, 2010b, *Gao et al.*, 2011]. Mixing in this model is parameterized by the Mellor-Yamada level 2.5 turbulence submodel as a default setup [*Mellor and Yamada*, 1982] with options of the General Turbulence Model (GOTM) [*Burchard*, 2002] in the vertical and the Smagorinsky turbulent parameterization [*Smagorinsky*, 1963] in the horizontal. The FVCOM used in this study is a fully 3-D wave-current coupled version. The wave model in FVCOM is SWAVE, an unstructured-grid version of SWAN solved by a second-order approximate semi-implicit finite-volume discrete method [*Qi et al.*, 2009]. SWAVE is coupled with FVCOM through radiation stress and surface stress in the momentum equations and the

wave-current interaction functions in the bottom boundary layer (BBL) [*Wu et al.*, 2010]. The roughness used to calculate the wind stress at the sea surface is based on formulae given in *Donelan et al.* [1993]. The BBL code used in this coupling was adopted from the code developed by *Warner et al.* [2008] and converted to an unstructured-grid finite-volume version using the FVCOM framework.

2.1.3. SELFE

[11] SELFE is the Semi-implicit Eulerian-Lagrangian finite-element model developed originally by *Zhang and Baptista* [2008] and modified and improved by many others [*Burla et al.*, 2010; *Bertin et al.*, 2009; *Brovchenko et al.*, 2011]. SELFE utilizes a semi-implicit time stepping in conjunction with a Eulerian-Lagrangian method (ELM) to treat advection terms, with improvements in grid flexibility and implementing a hybrid terrain-following topography coordinates and higher-order discrete algorithms for elevation [*Zhang and Baptista*, 2008]. The default numerical scheme is second-order accurate in space and time, with options for higher-order schemes. The SELFE used in this study is a fully current-wave coupled 2-D vertically integrated version. The surface wave model implemented into SELFE is WWM [*Roland*, 2009]. WWM incorporates the framework of residual distribution schemes [*Abgrall*, 2006] within a hybrid fractional splitting method utilizing third-order Ultimate Quickest schemes in spectral space, as also used by *Tolman* [1992] in the Wave Watch III (WWIII) model, and robust and accurate integration of the source terms based on a multiple splitting technique using TVD-Runge Kutta schemes for shallow water wave breaking and bottom friction, dynamic integration of the triad interaction source term and semi-implicit integration of the deep water physics. Coupling of WWM with SELFE was done through the radiation stress formulations according to *Longuet-Higgins and Stewart* [1964], the wave boundary layer (WBL) based on the theory of *Grant and Madsen* [1979], surface mixing following *Craig and Banner* [1994], and the current-induced Doppler shift for waves [*Komen et al.*, 1996].

[12] In this testbed experiment, FVCOM was run with its original 3-D setup, while ADCIRC and SELFE were run using their 2-D depth averaged formulation. The intermodel comparisons were made using the vertically averaged water transports and surface elevation. In ADCIRC and SELFE, the bottom friction was parameterized using Manning's n formulation with the bottom stress $(\tau_{bx}, \ \tau_{by})$ given as a quadratic slip boundary condition in the form of

$$(\tau_{bx}, \ \tau_{by}) = \rho C_f(U, \ V)\sqrt{U^2 + V^2} \qquad (1)$$

where U and V are the x- and y-components of vertically averaged velocity and C_f is the bottom drag coefficient given as

$$C_f = \frac{gn^2}{\sqrt[3]{h}} \qquad (2)$$

where g is the gravitational constant, n is the Manning roughness, and h is the total water column depth. In ADCIRC, n was specified as a variable parameter with a minimum value of 0.025 in open water and a maximum

value of 0.12 on land. In SELFE, n was specified as a constant parameter of 0.08 inside the harbor and 0.01 outside the harbor. In FVCOM, the bottom stress is also calculated by a quadratic formula in the form of

$$(\tau_{bx}, \ \tau_{by}) = \rho C_d(u_b, \ v_b)\sqrt{u_b^2 + v_b^2} \qquad (3)$$

where u_b and v_b are the x- and y-components of the bottom velocity and C_d is the bottom drag coefficient that is determined by matching a logarithmic bottom layer to the model at a height z_b above the bottom, i.e.,

$$C_d = \max\left[\frac{\kappa^2}{\ln\left(\frac{z_b}{z_o}\right)^2}, \ 0.0025 \right], \qquad (4)$$

where κ is the von Karman constant and z_o is the bottom roughness parameter. In the Scituate Harbor where the water depth is shallower than 40 m, $z_o = 0.003$ m.

2.2. Design of Numerical Experiments

[13] The testbed site Scituate is a coastal lagoon in Massachusetts Bay with a width of 195 m (between two breakwaters) at the mouth opening eastward onto the inner shelf (Figure 1). The water depth varies from ~15 m over the shelf to ~5–6 m in the deeper regions of the harbor, with a shallow and narrow connection to a wide area of wetland and salt marsh to the south. In the NECOFS pilot experiment, a subregional unstructured grid was created with a horizontal resolution varying from ~400–500 m over the shelf to ~10 m inside the harbor (Figure 2). In the vertical, a total of 10 uniform σ-layers were specified, with a vertical resolution varying from 1.5 m over the shelf to 0.1 m or less along the coast where the water depth is 1 m or shallower.

[14] Numerical experiments were made for the May 2005 and April 2007 storm events. In 2005, two nor'easters swept over the Massachusetts coast, the first during 5–10 May and the second during 24–27 May (Figure 3). The NDBC buoy 44013 located ~17 km NNE of Scituate in Massachusetts Bay reported maximum wind speeds >15 m/s during this period. Both storms caused significant inundation on the northern peninsula and at the southern end. The testbed experiments were focused on the second event. In 2007, a nor'easter occurred during 17–20 April. The wind direction and intensity of this storm were similar to the 24–27 May 2005 nor'easter event. The difference was that during the 24–27 May, 2005 nor'easter, the maximum wind lasted over high tide, while during 17–20 April, 2007, the maximum wind occurred during low tide.

[15] The experiments were made by running the three models with the same meteorological forcing and initial/boundary conditions for the entire month of May 2005 and April 2007, respectively. The surface wind and barometric pressure forcing used to drive the models were taken from hindcasts made with the NECOFS Gulf of Maine regional mesoscale weather models (MM5 for 2005 and WRF for 2007); we assimilated all available NDBC and coastal weather data in improve the mesoscale hindcasts. MM5 is the fifth-generation NCAR/PSU nonhydrostatic, terrain-
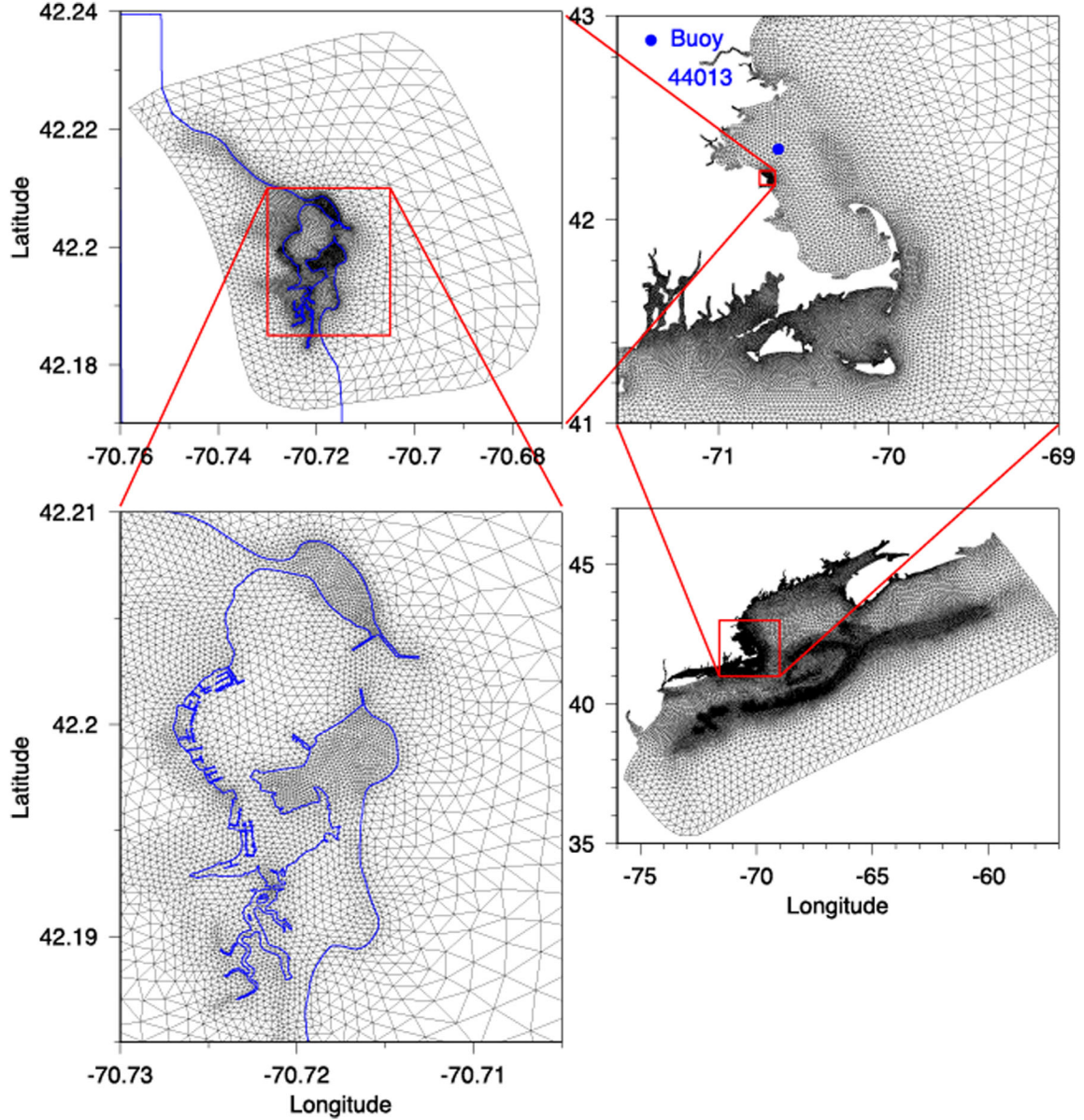
Figure 2. Unstructured triangular grid of the Scituate-FVCOM inundation system (top left) that is nested with the regional GM-FVCOM (bottom right). The top right figure is a zoomed view of the Massachusetts coast bounded by the red box shown in the GM-FVCOM grid. The blue dot is the location of NDBC 44013. The bottom left figure is a zoomed view of the Scituate Harbor grid bounded by the red box shown in the Scituate-FVCOM in the top-left figure.

following, sigma-coordinate mesoscale weather model developed jointly by the National Center for Atmospheric Research (NCAR) and Pennsylvania State University (PSU) [*Dudhia et al.*, 2003]. WRF is the newer Weather Research and Forecast model (with the same dynamics as MM5) developed by the NCEP/NCAR [*Skamarock and Klemp*, 2008] that we used to replace MM5 in NECOFS in 2006. The Scituate-FVCOM inundation model is nested with the NECOFS regional Gulf of Maine FVCOM model (GM-FVCOM). In this study, Scituate-FVCOM was spun up 1 month before the testbed model experiment runs started, and the model-predicted fields at the beginning of 1 May 2005 and 1 April 2007 were used as the initial condi-

tions for the three models. The open boundary forcing was also provided by GM-FVCOM, which has the same grid cells around the boundary zone of the Scituate-FVCOM mesh. This forcing includes the real-time sea level elevation (with both tidal and subtidal components) at boundary nodes and 3-D velocities in the centroid of boundary triangles.

[16] To help us examine the role of current-wave interaction in coastal inundation, we ran the three models for cases without and with inclusion of waves for the 2005 and 2007 nor'easter experiments. The SWAN, SWAVE, and WWM coupled with these three models were run with the same wave parameters listed in Table 1. To evaluate the
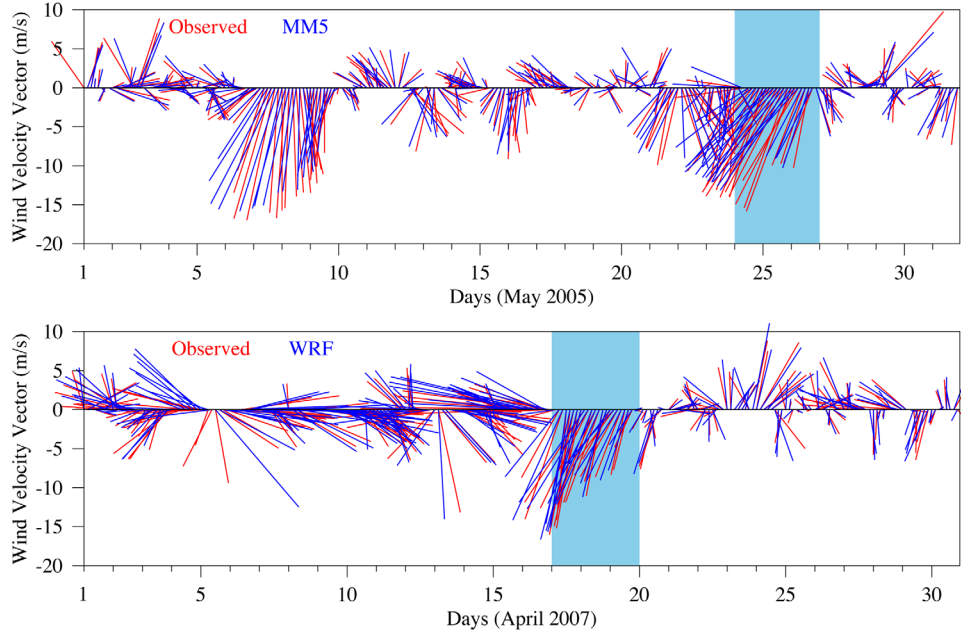
Figure 3. Observed (red) and modeled (blue) wind velocity vectors at the 10 m height at NDBC 44013 over 1–31 May 2005 and 1–30 April 2007, respectively. The blue shaded region marks the period during which the nor'easter was defined.

feedback effects of current-wave interaction to the surface waves, we also compared the wave model results for the cases without and with coupling to the hydrodynamic models. In the following sections, we define these four experiments as follows: Experiment 1—the hydrodynamic model run without inclusion of waves; Experiment 2—the wave-current coupled model run; Experiment 3—the surface wave simulation without coupling to the hydrodynamic model; and Experiment 4—the surface wave simulation with inclusion of wave-current interaction. For brevity, we will use the term "with waves" to indicate simulations made with wave-current interaction included, and the term "without waves" to mean simulations made without coupling the wave and hydrodynamic models.

3. Simulation Results

3.1. Tidal Simulation

[17] In 2010, the Taunton WFO installed a tide gauge in Scituate Harbor to help improve their inundation forecasting. To validate the three models, we selected May 2010 as the test period to compare model-predicted tides with observations. This is a prerequisite for an inundation model since large inundation usually occurs at or near high tide. For the tidal simulation, each model was forced at the open

boundary by elevation time series constructed using the five major tidal constituents (M_2, N_2, S_2, O_1, and K_1). The tidal constants (amplitude and phase) for these constituents were computed for the 1–31 May 2010 period using the MATLAB harmonic analysis toolbox T_Tide [*Pawlowicz et al.*, 2002]. The resulting model elevation time series were then analyzed using T_Tide and the tidal constants compared.

[18] For the same boundary tidal forcing, the three models provided similar accuracy for tidal elevation (Tables 2 and 3), with a root-mean-square (RMS) error of ∼ 8.0 cm over the entire month. The difference with observations occurred mainly in tidal phases, which is believed to be due to the bottom friction parameterization used in the models. ADCIRC and SELFE were run using their 2-D version in which bottom friction was parameterized by the Manning formulation with different Manning n coefficients, while FVCOM was run using its 3-D version in which bottom friction was parameterized through a bottom log-profile viscous layer. Since sea level inside Scituate Harbor changed almost simultaneously, however, the different bottom friction formulations used in the three models showed little influence on model performance in simulating tidal phase, and the model-computed errors were in or close to uncertainties of observations.

3.2. Inundation

[19] To examine the impact of current-wave interaction on storm-induced inundation, we compared the total inundated areas predicted by ADCIRC, FVCOM, and SELFE for the cases without waves and with waves. In general, more severe flooding occurred in the 2005 event than in the 2007 event, and in the cases with waves than without waves. In the 2005 event, for the case without waves, the three models agreed well on the spatial distributions of the

Table 1. Wave Parameters Used in SWAN, SWAVE, and WWM

Direction	Full Circle
Direction bins (number)	36
Frequency bins (number)	24
Lowest discrete frequency (Hz)	0.05
Highest discrete frequency (Hz)	0.5
Bottom friction formulation	Jonswap
Minimum water depth for wet/dry treatment (m)	0.05

Table 2. Comparison for Observed and Computed Tidal Amplitudes at the Scituate Tide Gauge

	OBS (m)	ADCIRC (m)	Difference (m)	FVCOM (m)	Difference (m)	SELFE (m)	Difference (m)
M2	1.32 ± 0.03	1.24 ± 0.02	-0.08	1.24 ± 0.02	-0.08	1.24 ± 0.03	-0.08
N2	0.25 ± 0.03	0.28 ± 0.02	0.03	0.28 ± 0.02	0.03	0.28 ± 0.03	0.03
S2	0.17 ± 0.03	0.19 ± 0.02	0.02	0.19 ± 0.02	0.02	0.19 ± 0.02	0.02
O1	0.12 ± 0.01	0.11 ± 0.01	-0.01	0.11 ± 0.01	-0.01	0.11 ± 0.01	-0.01
K1	0.14 ± 0.01	0.13 ± 0.01	-0.01	0.13 ± 0.01	-0.01	0.13 ± 0.01	-0.01

flooded area. Protected by seawalls along the coast, no overtopping appeared along the coast outside of Scituate Harbor. Inside the harbor, three major flooded areas were predicted: (1) on the northern peninsula, where water flowed onto the back side through a narrow channel, (2) the western coast of the southern peninsula connected to the mouth of the harbor, and (3) at the southern end, where water entered the large wetland and marsh area through two narrow tidal creeks (Figure 4, top). Adding wave-current interaction resulted in relatively larger flooding at the southern end and slightly more flooded area on the northern peninsula (Figure 4, bottom). On the northern peninsula, ADCIRC- and FVCOM-predicted flooded areas were very similar for the case without waves, while FVCOM and SELFE were similar for the case with waves. The three model-predicted flooded areas on the western coast of the southern peninsula remained the same for both cases without and with waves. At the southern end, after wave-current interaction was included, ADCIRC showed that the flooded area was significantly enlarged, but not in FVCOM and SELFE.

[20] In the 2007 event, for the cases without waves, no significant flooding occurred on the northern peninsula and at the southern end except on the western coast of the southern peninsula (Figure 5, top). In that area, no significant difference was shown in the inundation areas predicted by the three models. When waves were included, all three models predicted flooding on the northern peninsula and at the southern end (Figure 5, bottom). At the southern end, the flooded area predicted was larger in FVCOM than in ADCIRC and SELFE.

[21] The three models all suggest that inundation was greater in the 2005 event than in the 2007 event, independent of whether or not wave-current interaction was included. In the 2005 event, the strong northeasterly wind appeared around 14:00 GMT 24 May and lasted until 00:00 GMT 26 May. The largest inundation occurred at high tide around 5:00 GMT 25 May. In the 2007 event, the wind was strongest around 18:00–22:00 GMT 17 April during the ebb tidal phase. Although the wind had the same amplitude as that observed in May 2005 nor'easter, no significant inundation occurred during the strongest wind pe-

riod due to the canceling effect of the wind-induced onshore transport by the tidal-induced offshore transport through the harbor entrance. Although small, the maximum inundation occurred around 4:00 GMT at high tide on May 28, at which time the wind was about 5 m/s lower than the maximum wind. Inside Scituate Harbor, with the inclusion of current-wave interaction, the significant wave heights predicted by the three models were in phase as the tidal elevation. This is the reason why adding wave-current interaction resulted in more significant inundation. In the 2005 event, the strongest wind co-occurred with high tide, resulting in significant flooding without the need for including wave-current interaction. In the 2007 event, the strongest wind occurred during the ebb tide so that adding wave-current interaction played a critical role in producing significant flooding.

[22] Using the same mesh configuration, surface forcing, and initial/boundary conditions, the difference was still noticeable in the inundation results for ADCIRC, FVCOM, and SELFE (Table 4). In the 2005 event, the model-predicted inundation area was largest in FVCOM and smallest in SELFE. The difference was 0.03 km^2 between FVCOM and ADCIRC (15% larger in FVCOM), 0.06 km^2 between FVCOM and SELFE (35% larger in FVCOM), and 0.03 km^2 between ADCIRC and SELFE (18% larger in ADCIRC) for the cases without waves. Although the wave models implemented in the three models were different, the contributions of current-wave interaction to the flooded area were similar in the 2005 event. The inundation area was enlarged by 0.03 km^2 for FVCOM (13% larger) and SELFE (18% larger) and by 0.05 km^2 for ADCIRC (25% larger). In the 2007 event, the flooded areas predicted by the three models were very close for the cases without waves, while the flooded area was enlarged by 0.07 km^2 in FVCOM (64% larger) and ADCIRC (70% larger), and 0.04 km^2 in SELFE (40% larger) with wave-current interaction. The enlarged rates of FVCOM and ADCIRC were the same. Since no quantitative measurements were made of the flooded area, we were not able to evaluate the accuracy of the three models. We believe that the small intermodel differences were caused by the different algorithms and criterions used to estimate the flooding/drying process and the

Table 3. Comparison for Observed and Computed Tidal Phases at the Scituate Tide Gauge

	OBS (°)	ADCIRC (°)	Difference (°)	FVCOM (°)	Difference (°)	SELFE (°)	Difference (°)
M2	103.46 ± 1.36	101.62 ± 0.97	-1.84	101.66 ± 0.94	-1.80	101.97 ± 1.05	-1.49
N2	68.62 ± 8.03	69.58 ± 4.57	0.96	69.51 ± 4.66	0.89	69.87 ± 4.52	1.25
S2	141.30 ± 12.83	152.58 ± 7.09	11.28	152.81 ± 6.81	11.51	153.17 ± 6.99	11.87
O1	187.13 ± 5.63	183.49 ± 2.27	-3.64	183.56 ± 2.11	-3.57	183.59 ± 2.70	-3.54
K1	198.77 ± 4.64	193.53 ± 1.98	-5.24	193.48 ± 2.00	-5.29	193.93 ± 2.20	-4.84

ADCIRC FVCOM SELFE
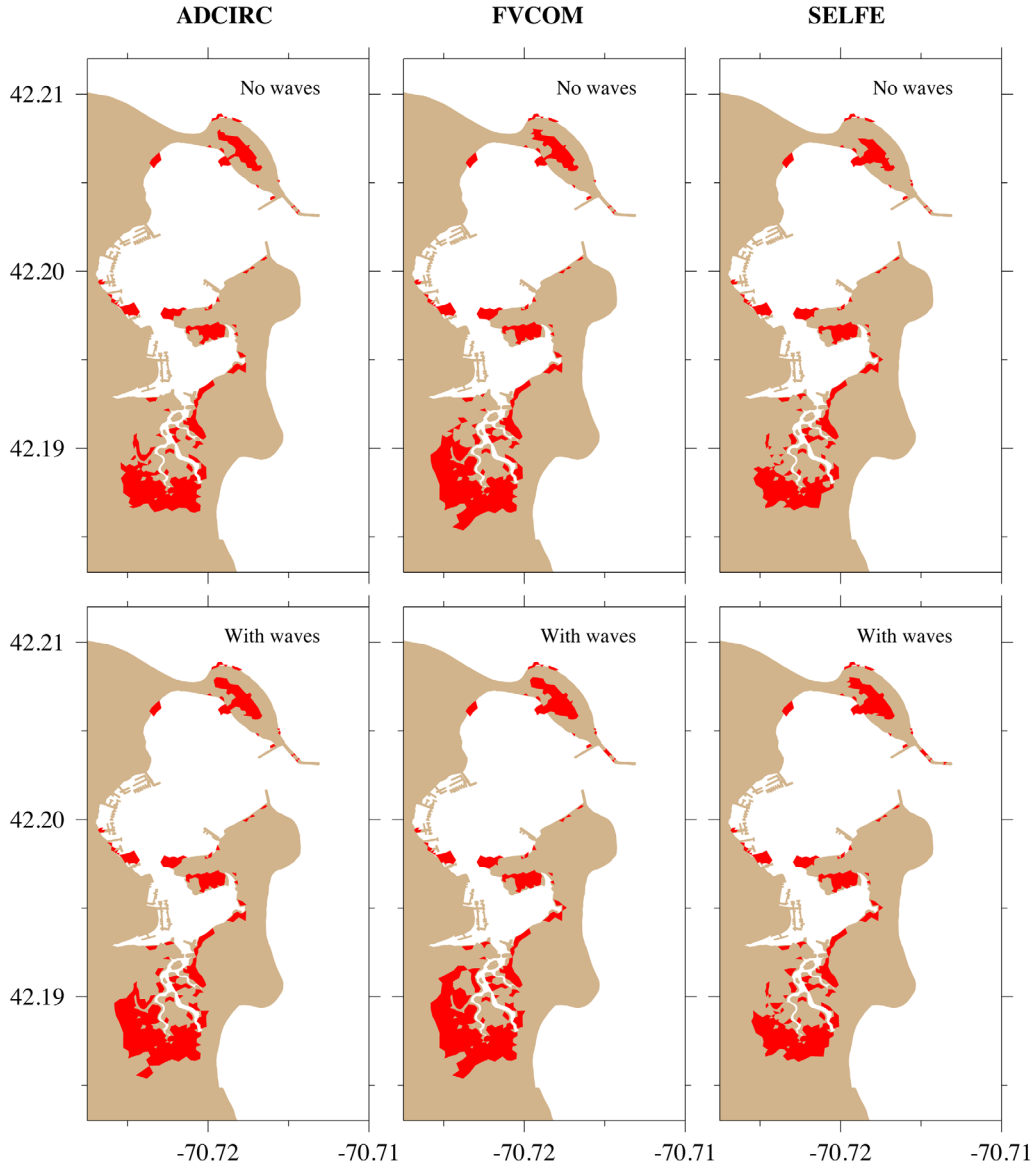
Figure 4. The total flooded areas predicted by ADCIRC (left), FVCOM (middle), and SELFE (right) for the cases without (top) and with (bottom) wave-current interaction during the May 2005 nor'easter storm event.

parameterizations used for bottom friction parameterizations used in these 3-D and 2-D models.

3.3. Water Currents

[23] The three models predicted similar spatial and temporal patterns of water currents in both cases without and with wave-current interaction. Examples are shown in Figures 6 and 7 for snapshots of the vertically averaged current taken at 05:00 GMT 25 May 2005 and 04:00 GMT 18 April 2007, respectively. In both 2005 and 2007 events, for the cases without wave-current interaction, the models show that the northeasterly wind produced a relatively strong southward along-shelf current over the shelf, a weak anticyclonic separation eddy in the harbor entrance behind the easternmost breakwater, and the same order of magnitude weakly cyclonic circulation inside the harbor. When wave-current interaction was included, the along-shelf cur-

rent was strongly intensified over the shelf. On the shelf off the northern peninsula, the current turned toward the coast, creating a stagnation point. This onshore current diverged at the coast, creating strong northwestward and

Table 4. Total Maximum Inundated Areas Predicted by ADCIRC, FVCOM, and SELFE for the 2005 and 2007 Nor'easters

| Case	ADCIRC (km²)	FVCOM (km²)	SELFE (km²)
	May 2005 Nor'easter		
No Waves	0.20	0.23	0.17
With Waves	0.25	0.26	0.20
	April 2007 Nor'easter		
No Waves	0.10	0.11	0.10
With Waves	0.17	0.18	0.14

8
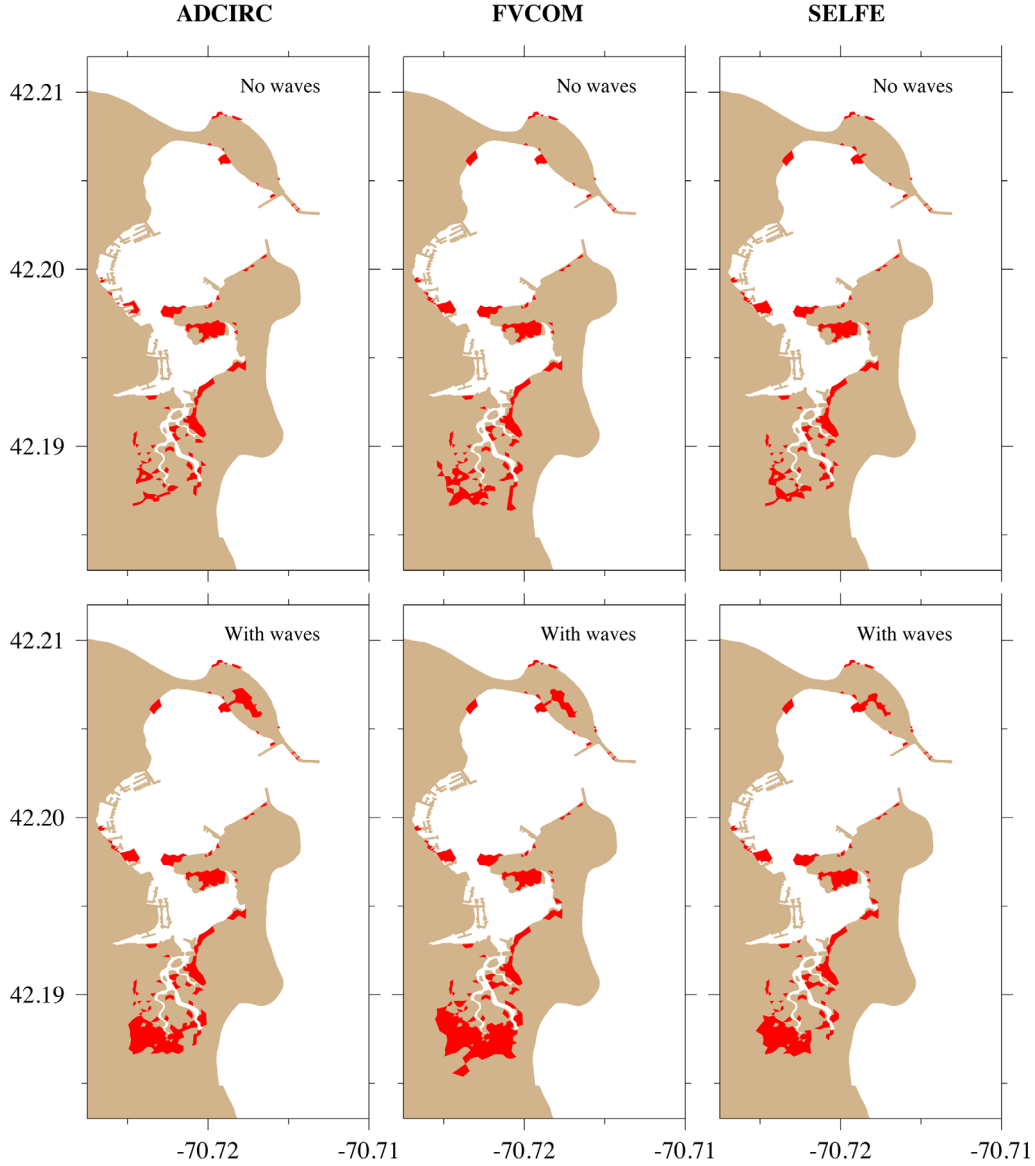
Figure 5. The total flooded areas predicted by ADCIRC (left), FVCOM (middle), and SELFE (right) for the cases without (top) and with (bottom) wave-current interaction during the April 2007 nor'easter storm event.

southward along-shelf currents around that area and around the harbor entrance and along the southern peninsula. The anticyclonic eddy in the harbor entrance was also intensified, with speeds up to the same order of magnitude as the currents over the shelf. The currents within the harbor remained relatively weak. All three models consistently showed that wave-current interaction could not only significantly enhance the current but also change the current direction over the shelf and entrance. This result is consistent with *Signell and List* [1997], who found that wave-current interaction could increase (reduce) the cross-shelf (along-shelf) storm-driven transport as a result of an increase in the effective bottom friction in Massachusetts Bay.

[24] The differences among ADCIRC, FVCOM, and SELFE were evident mainly in the current magnitudes over the shelf. In both the cases without and with waves,

SELFE-predicted currents (shown in Figures 6 and 7) were relatively weaker than those predicted by ADCIRC and FVCOM. For the cases without waves, in the 2005 event, FVCOM predicted a relatively strong flow along the shelf off the northern peninsula. This current was visible in ADCIRC, even though its magnitude was relatively weak. ADCIRC showed a relatively stronger current than FVCOM on the southern shelf. The same difference was found in the 2007 event, and the currents on the northern shelf showed an opposite direction between ADCIRC and FVCOM. For the case with wave-current interaction, ADCIRC- and FVCOM-predicted currents were very similar, particularly for the eddy intensification in the entrance mouth and divergent flow on the northern shelf and intensified flow on the southern shelf.

[25] It should be pointed out here that FVCOM was run as a 3-D model through nesting to the regional
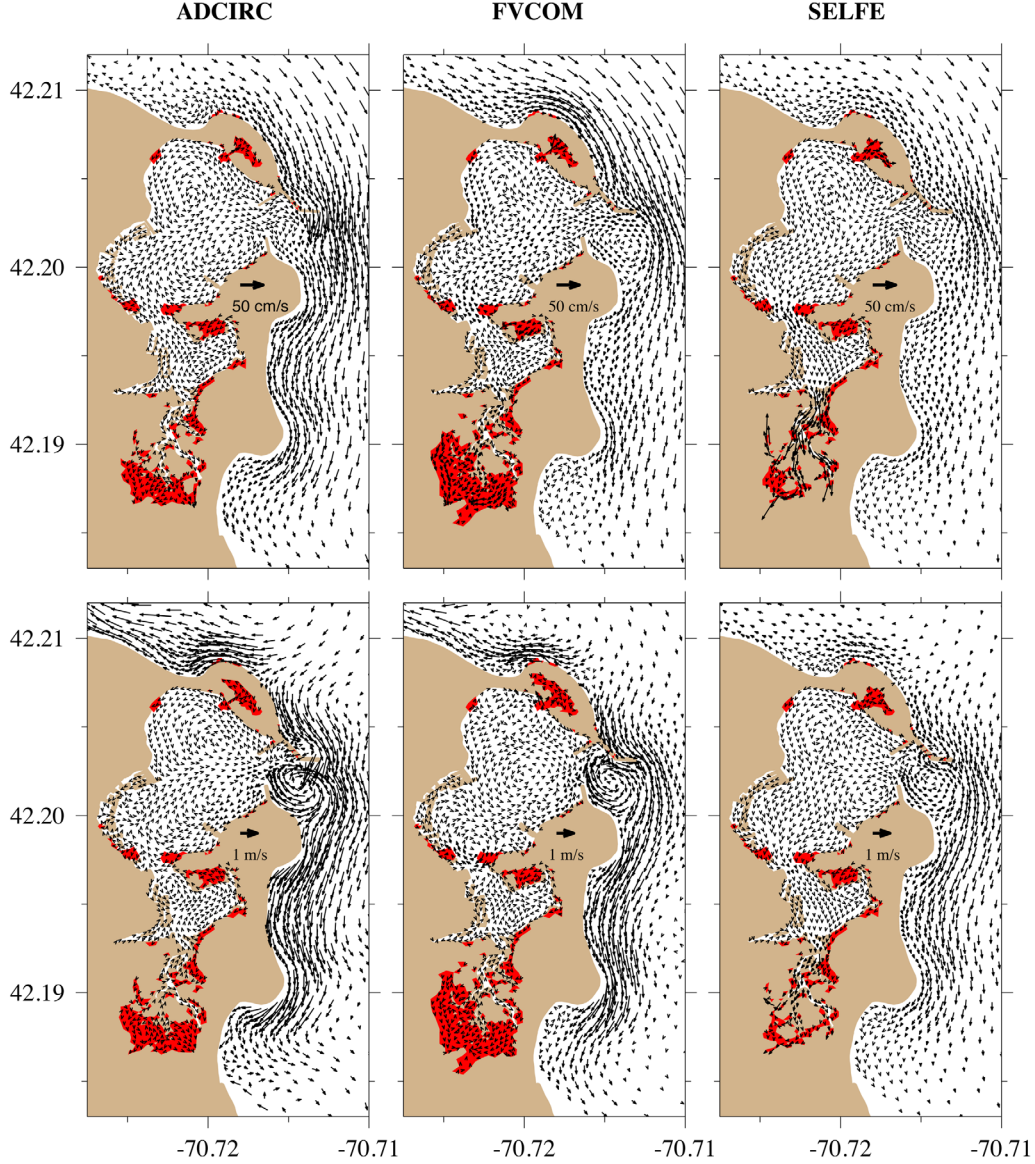
Figure 6. Snapshots of vertically averaged current vectors and inundation areas (red) predicted by ADCIRC (left), FVCOM (middle), and SELFE (right) at 05:00 GMT 25 May 2005 for the cases without (top) and with (bottom) wave-current interaction.

GM-FVCOM with volume and mass conservation between the two domains. The nesting boundary conditions included both sea level elevation and water velocity. ADCIRC and SELFE were forced by the boundary conditions provided by FVCOM. Since the velocity is placed at nodes in ADCIRC, at the centroids in FVCOM, and at the midpoint of the side lines of a triangle in SELFE, an interpolation approach was required to apply the FVCOM velocity nested boundary into ADCIRC and SELFE. This treatment could affect the current simulation results over the shelf. It is likely that the boundary issues did not influence the simulations of water level inside the harbor (see the discussion in the following sections).

3.4. Water Elevation and Flux Time Series

[26] We have compared time series of the water elevation at selected sites A-F and the water flux through trans-

ects a1-a2, b1-b2, and c1-c2 (see Figure 1) for both the 2005 and 2007 events (Figures 8 and 9). We have also compared the vertically averaged currents at sites A-F. However, since the three models compute velocity at different points in the triangular element, direct comparison of the model velocities at a single point required spatial interpolation, thus making the results sensitive to the interpolation method. To avoid confusion, we have not included here direct velocity comparisons.

[27] At sites A–E, in both cases without and with wave-current interaction, the only significant intermodel differences in water elevation were found in the timing of drying. In the 2005 event, for example, at site A, the water level difference at 05:00 GMT 25 May was 0.5 cm between ADCIRC and FVCOM, and 3.5 cm between ADCIRC and SELFE. At site E (the entrance to the southern end), the difference at the same time was 0.8 cm between ADCIRC

ADCIRC   **FVCOM**   **SELFE**
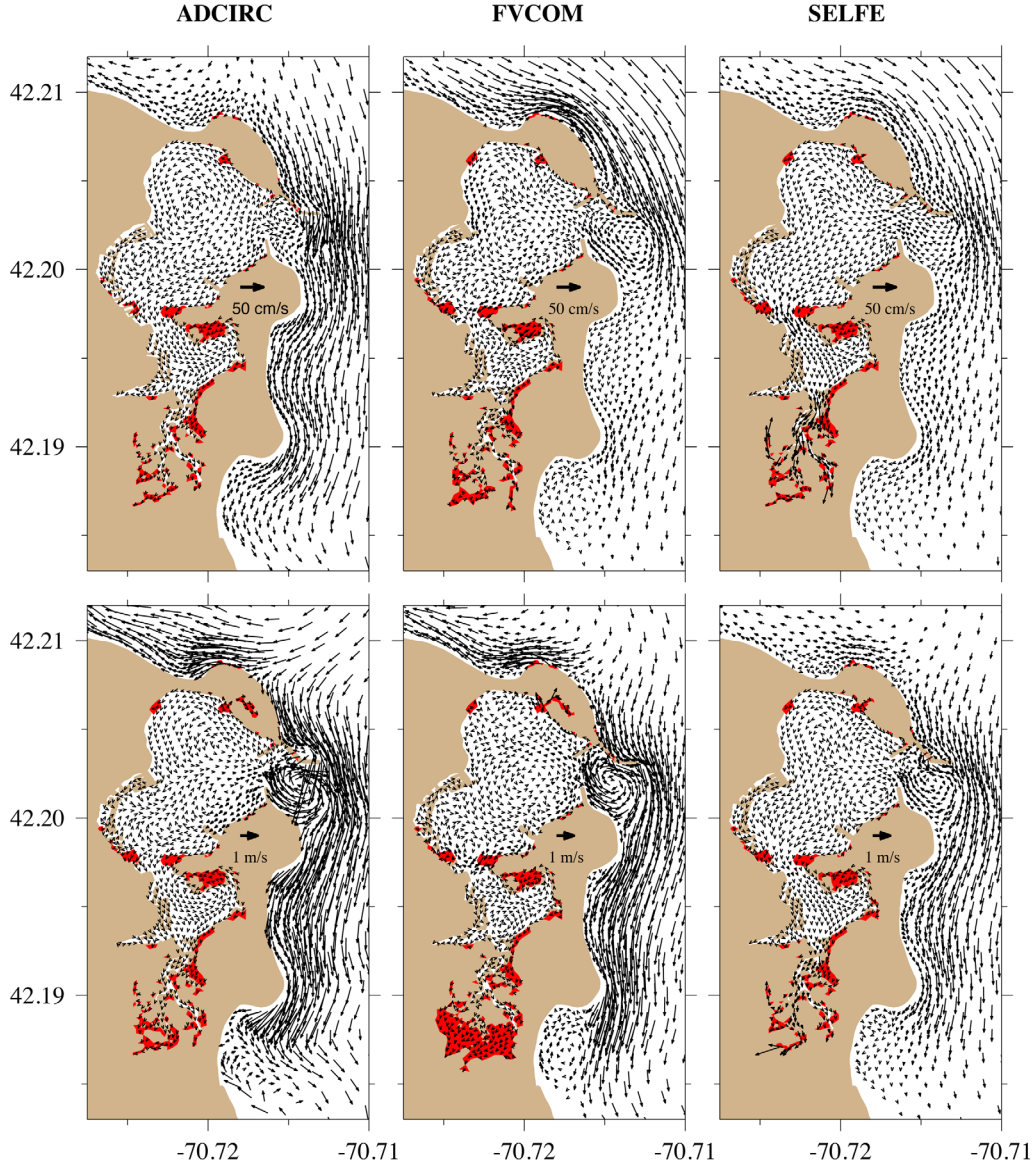
Figure 7. Snapshots of vertically averaged current vectors and inundation areas (red) predicted by ADCIRC (left), FVCOM (middle), and SELFE (right) at 04:00 GMT 18 April2007 for the cases without (top) and with (bottom) wave-current interaction.

and FVCOM and 1.1 cm between ADCIRC and SELFE. The different timing of drying shown among ADCIRC, FVCOM, and SEFLE is not surprising, since the three models use different criterions for determining wet/dry grid cells.

[28] A big difference appeared at site F on the northern peninsula. The land height at that point is 1.84 m. In the 2005 event, for the case without wave-current interaction, ADCIRC and FVCOM showed that site F was dry until 04:00 GMT 25 May and flooded over the water height of ∼20 cm at 05:00 GMT 25 May. This flooding event also appeared in the SELFE result, but the water height was only ∼4 cm. All three models showed a second event at 05:00 GMT 26 May, at which time the ADCIRC- and FVCOM-predicted sea levels were almost the same, but SELFE was ∼11 cm lower. ADCIRC and FVCOM showed that adding wave-current interaction did not change the

timing of flooding but did enlarge the flooded area with a rise of water level of ∼20 cm. This feature was also evident in SELFE, but the water level at 05:00 GMT was lower than ADCIRC and FVCOM. In the 2007 event, all three models were consistent for the case without wave-current interaction; no flooding occurred at site F! For the case with wave-current interaction, ADCIRC and FVCOM predicted two inundation events: one at 05:00 GMT 18 April and another at 06:00 GMT 19 April, while SELFE remained "dry" at site F. For this case, ADCIRC-predicted flooding water level was ∼24 cm higher than FVCOM.

[29] Transects a1-a2, b1-b2, and c1-c2 were made across the harbor entrance, the west coast of the northern peninsula, and the water passages entering the southern end (Figure 1). On transect a1-a2, the water flux predicted by the three models varied with the dominant M_2 tidal cycle (Figure 10). For the 2005 event, the flux difference
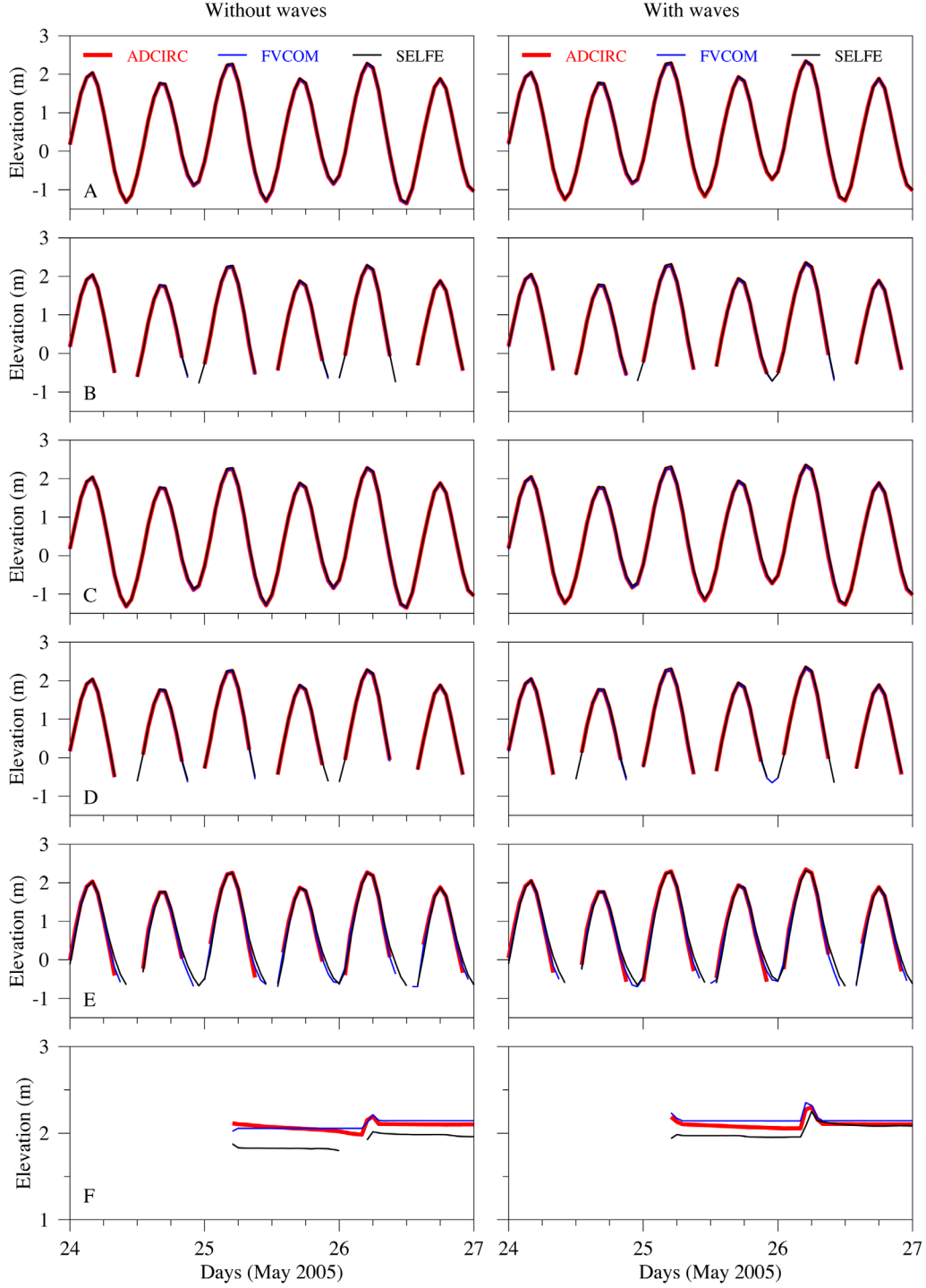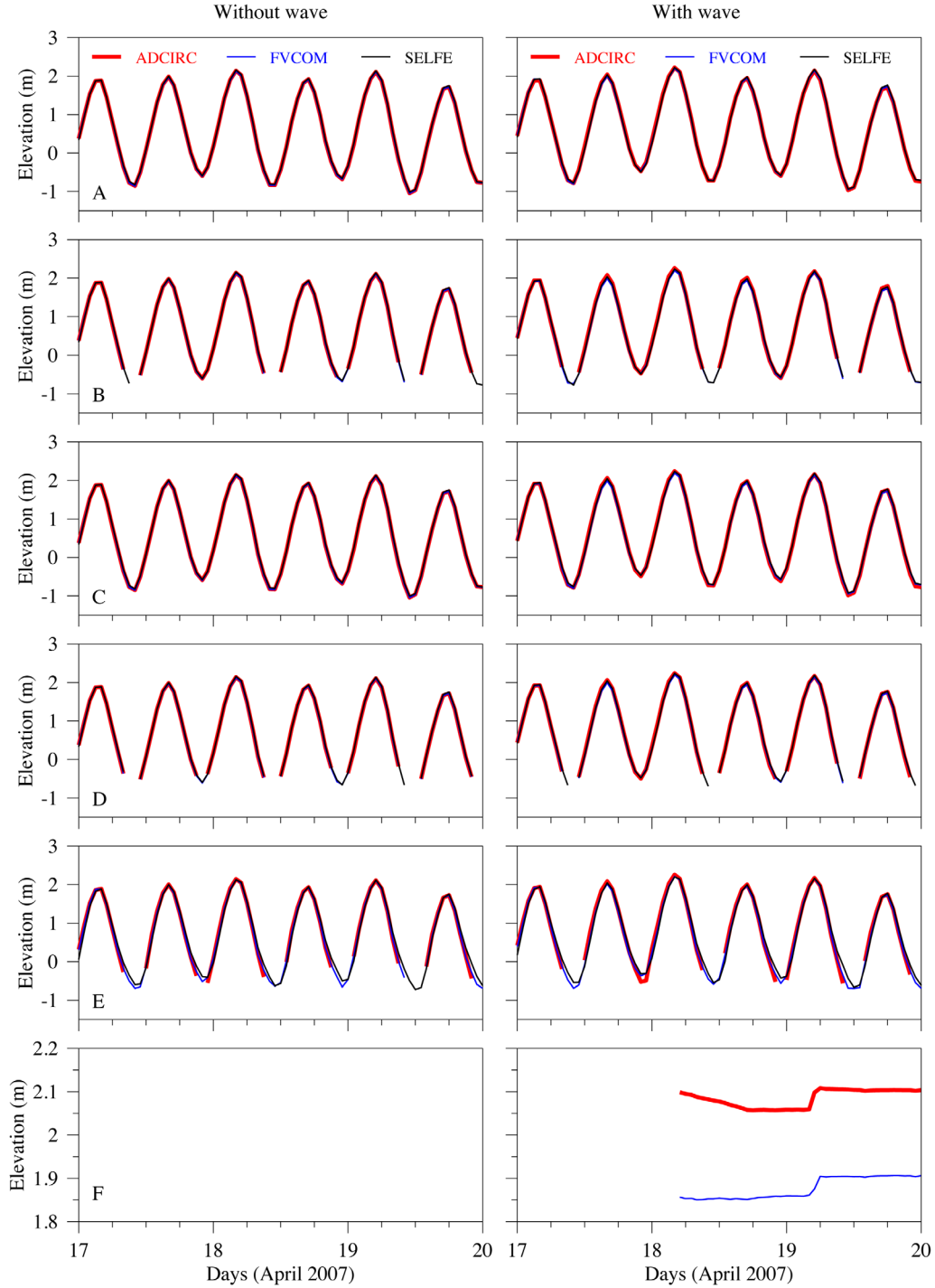
Figure 8. Comparisons of the time series of water elevation predicted by ADCIRC, FVCOM, and SELFE at sites A–F during 24–27 May 2005 for the cases without (left) and with (right) wave-current interaction.

between the cases without and with waves [of order 40 m³/s (~20%) or less] occurred primarily during the strong wind period (see Figure 3). The area of this transect is ~830 m², so that the maximum inflow increased by current-wave interaction during the storm was just ~5 cm/s, occurring at maximum flood tide. One common feature we learned using these three models is that wave-current interaction significantly enhanced the anticyclonic eddy at the entrance of the harbor. Because of the existence of this eddy, wave-current interaction could increase the inflow during flood tide and the outflow during ebb tide. For this reason, coastal flooding inside the harbor was not considerably enlarged in the case with wave-current interaction in the 2005 event.
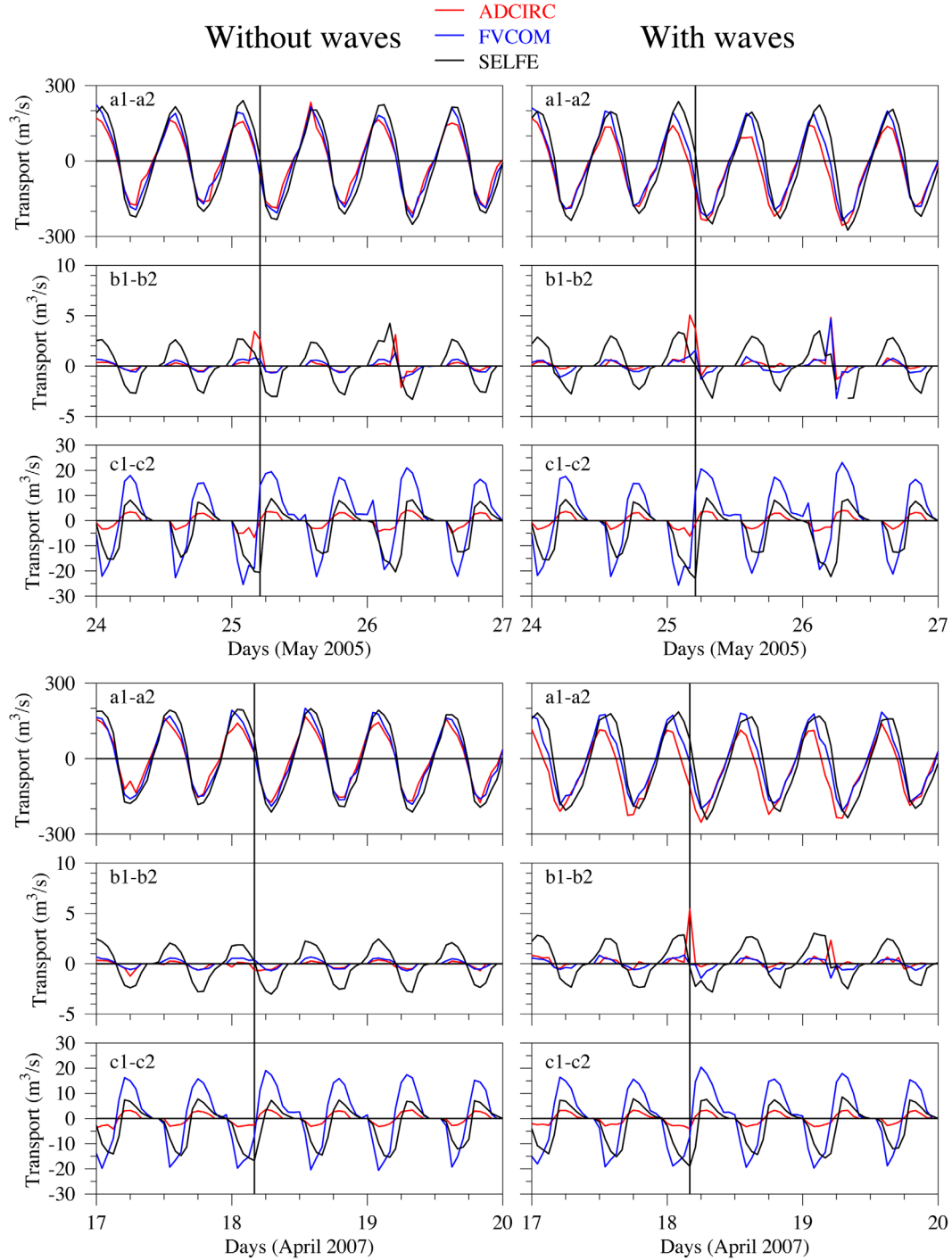
Figure 9. Comparisons of the time series of water elevation predicted by ADCIRC, FVCOM, and SELFE at sites A–F during 17–20 April 2007 for the cases without (left) and with (right) wave-current interaction. SELFE remained dry at F, no water elevation was represented.

[30] A similar difference was also detected in the 2007 event. Wave-current interaction enhanced the net flux into the harbor during flood tide and caused the inundation on the northern peninsula and enlarged the flooded areas in the southern end. The maximum inflow flux difference between the cases with and without waves was ∼45 m³/s (∼23%) for FVCOM, >50 m³/s (∼25%) for ADCIRC, and ∼15 m³/s (8%) for SELFE. In this case, FVCOM showed the largest flooding at the southern end (Figure 5) and highest water level there (Figure 9) while ADCIRC showed the highest water level at site F, indicating that wave-current interaction can cause the transport pattern within the harbor to differ between the three models, in addition to the criterion for wetting and drying employed by the three models.

[31] On transect b1-b2 on the western coast of the northern peninsula, both ADCIRC and FVCOM showed two

Figure 10. The water flux through transects a1-a2, b1-b2, and c1-c2 estimated by ADCIRC, FVCOM, and SELFE during 24–27 May 2005 and 17–20 April 2007 for the cases without (left) and with (right) wave-current interaction. Positive: inflow and negative: outflow. The black vertical line indicated when maximum flooding occurred.

peaks in the onshore water transport early on 25 and 26 May 2005 (Figure 10), consistent with the elevation time series shown in Figure 8. These two peaks were higher when wave-current interaction was included. Unlike ADCIRC and FVCOM, SELFE-predicted flux on this transect was about double that of ADCIRC and FVCOM and varied periodically with the tidal cycle. In both cases with-

out and with waves, the SELFE inflow and outflow were in the same order and timing as the maximum inflow fluxes on 25 and 26 May 2005 and occurred earlier than ADCIRC and FVCOM. The SELFE-predicted flux on transect b1-b2 seems to be consistent with the water elevation time series at site F (Figure 8), where minimal flooding appeared around 05:00 GMT 25 May but more significant flooding
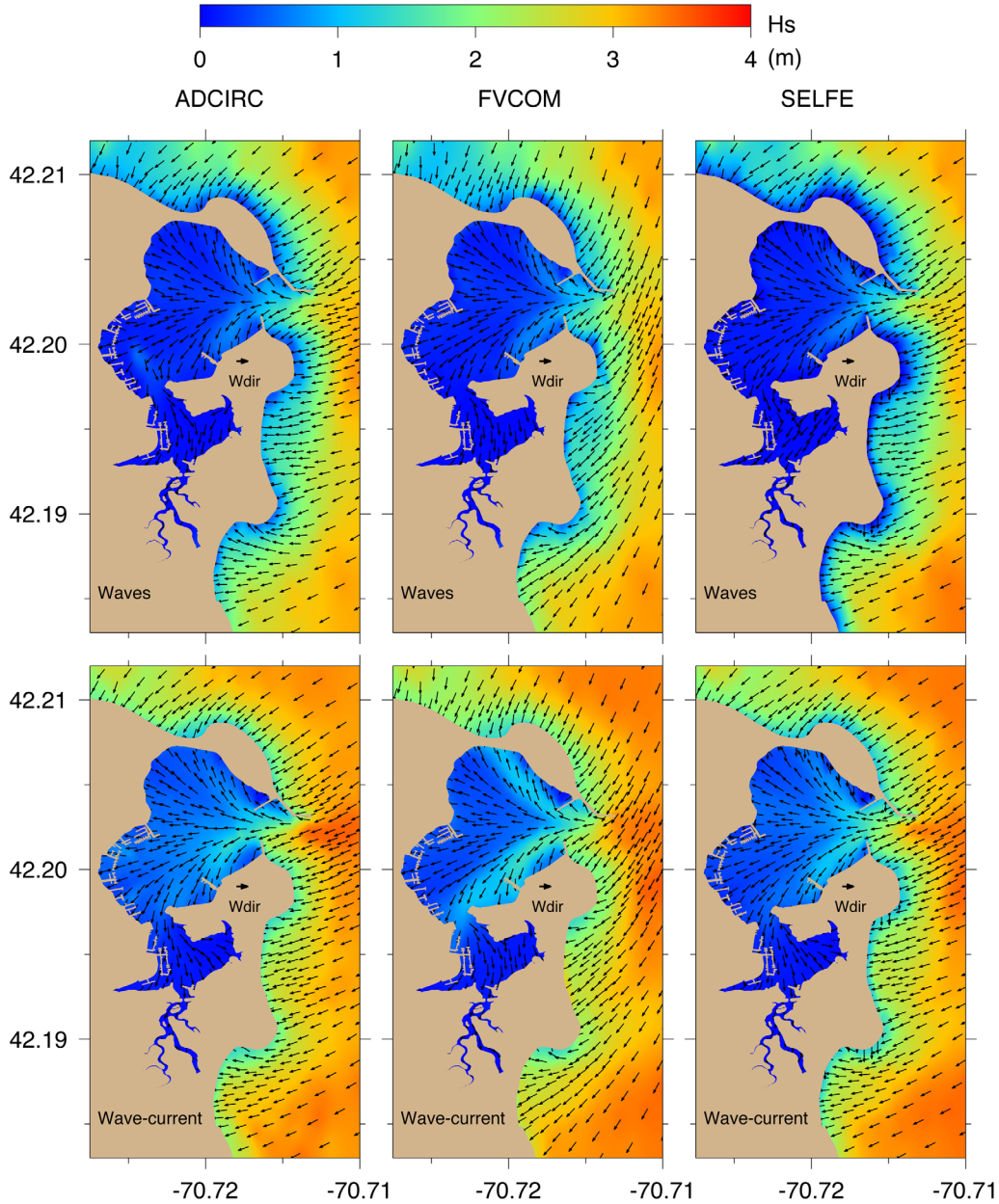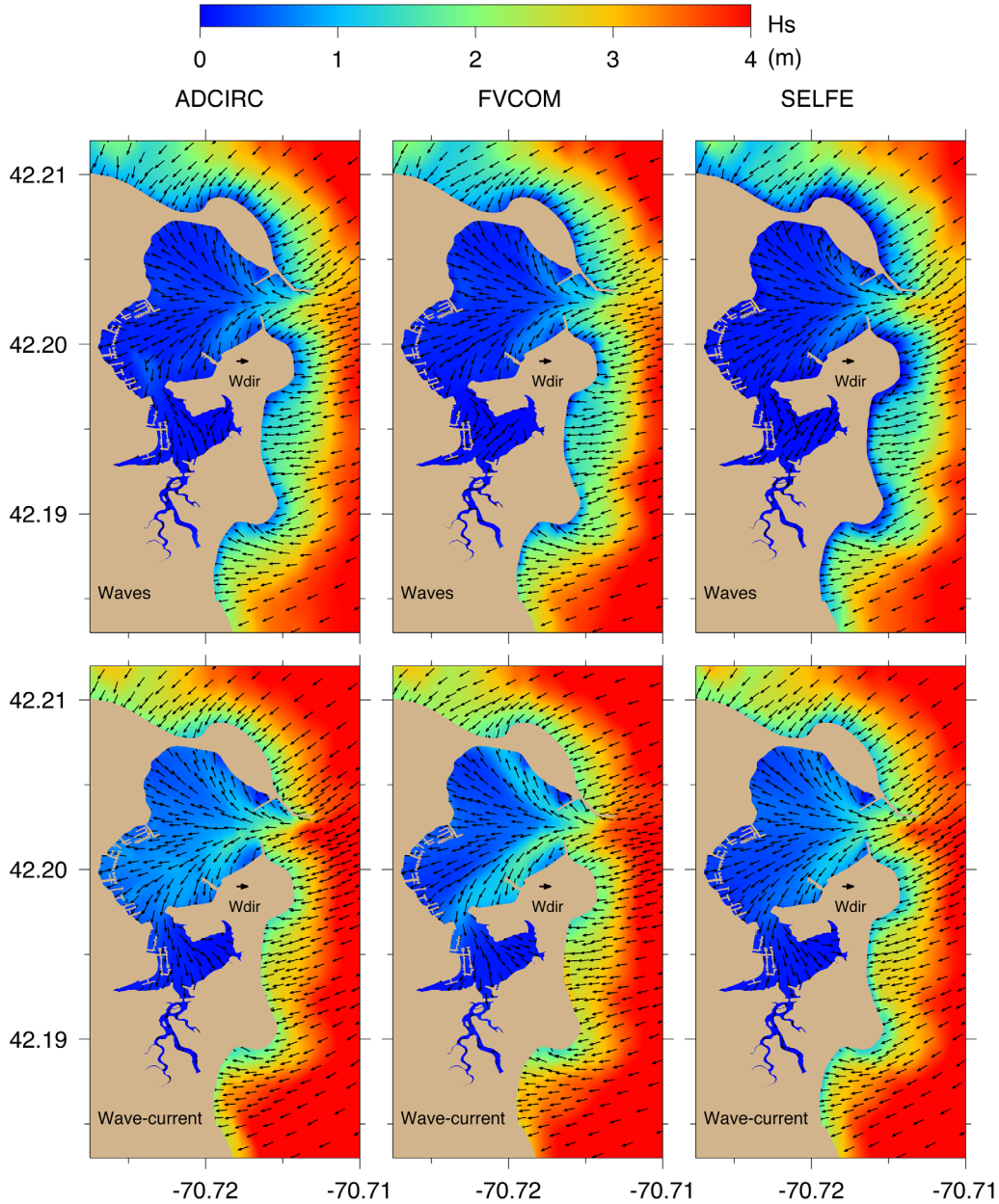
Figure 11. Snapshots of the significant wave height predicted by SWAN, SWAVE, and WWM at 05:00 GMT 25 May 2005 for the cases without (top) and with (bottom) wave-current interaction. Vectors: wave direction.

occurred around 05:00 GMT 26 May. Similar features were also found in the 2007 event. For the case without waves, the ADCIRC- and FVCOM-predicted fluxes were similar and very small, while the SELFE-predicted flux was roughly 1 order of magnitude larger, with slightly larger outflow than inflow. For the case with waves, the ADCIRC-predicted flux during the flooding periods in early 18 and 19 April were much larger than FVCOM and SELFE.

[32] On transect c1-c2, the three models showed that the timing of flooding was a few hours later than those found on transect b1-b2. For both 2005 and 2007 events, the southward flux predicted by FVCOM was about double that predicted by ADCIRC and SELFE. The three models showed similar phases during the flood tide but not during the ebb tide. The maximum peak of the outflow flux predicted by SELFE was a few hours delayed after the peak predicted by FVCOM and ADCIRC.

[33] We note here that it was difficult to compare quantitatively the volume fluxes calculated through these transects by the three models, since the results were sensitive to the algorithms used to calculate the flux. FVCOM uses a finite-volume algorithm designed to ensure flux conservation in a closed system, while ADCIRC and SELFE used algorithms that required interpolation of the velocity field. Applying these algorithms in regions of large currents with complex patterns and horizontal shears (e.g., the harbor entrance eddy) could lead to differing flux estimates.

Figure 12. Snapshots of the significant wave height predicted by SWAN, SWAVE, and WWM at 04:00 GMT 18 April 2007 for the cases without (top) and with (bottom) wave-current interaction. Vectors: wave direction.

4. Discussion

[34] The intermodel comparisons described above suggest that the primary difference in the performance of the three models occurred in the case with the inclusion of wave-current interaction. In the case with the same forcing, boundary/initial conditions, and grid configuration, we believe that the difference was mainly caused by different discrete algorithms used to solve the three wave models, compute wave-current interaction, and use the wet-dry point treatment for simulating inundation as well as different bottom friction parameterizations. The water elevations predicted by the three models were very close to each other at wet points but differed considerably at flooding sites,

suggesting that for the given same grid, forcing and initial/boundary conditions, the three models were all capable of simulating the change in water level at points in the harbor that were never dry. At flooding sites, however, since the wet/dry point treatment algorithms and criterions implemented in these models were different, with a certain level of dependence on empirical methods, we should not expect to see identical flooding predictions even through these methods were all validated via field measurements in previous applications [e.g., *Bunya et al.*, 2010; *Chen et al.*, 2007; *Zhang et al.*, 2011].

[35] One question was raised regarding the differences found in the case with wave-current interaction: Did the three models predict the same wave features in Scituate for
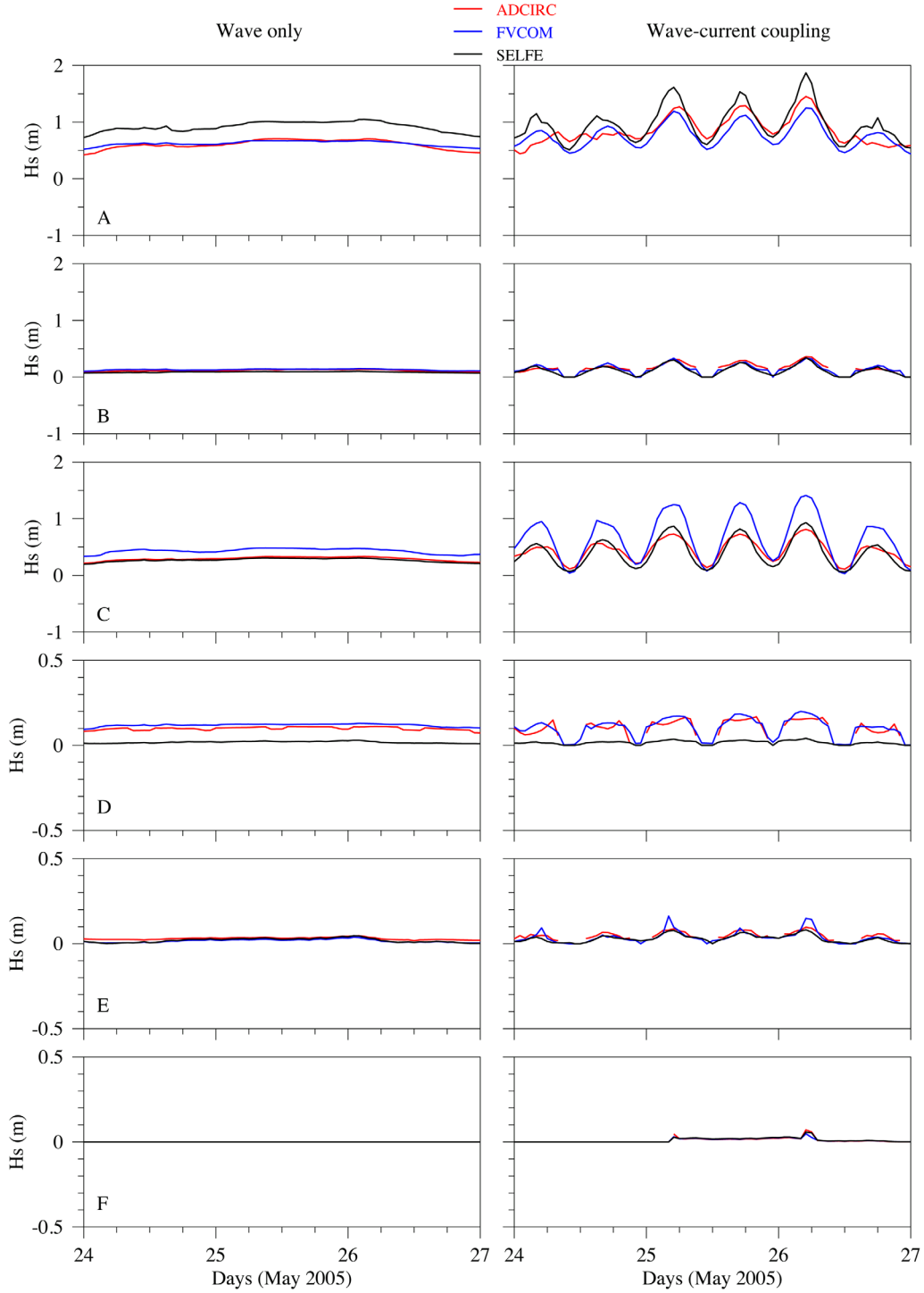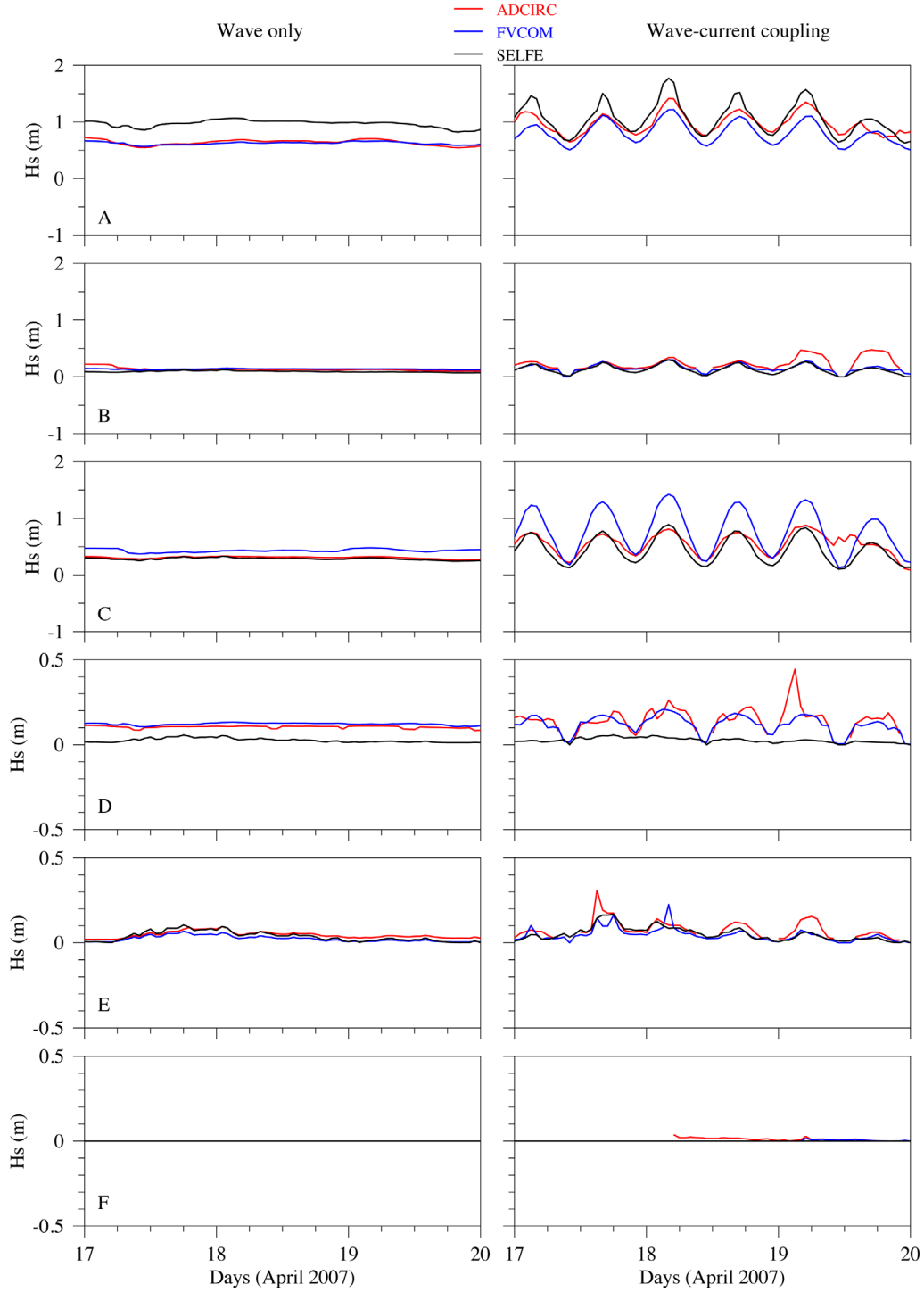
Figure 13. Comparisons of the time series of significant wave height predicted by ADCIRC (red), FVCOM (blue), and SELFE (black) at sites A-F during 24–27 May 2005 for the cases without (left) and with (right) wave-current interaction.

these two extratropical storms? If not, it suggests that these differences could be due to different performances of SWAN, SWAVE, and WWM (e.g., the algorithms used to calculate radiation stress and bottom friction). To investigate this question, we compared the spatial (snapshot) distributions and temporal (time series at sites) variation of significant wave height and peak frequency predicted by

SWAN, SWAVE, and WWM for the 2005 and 2007 events.

[36] These simulations were conducted without and with inclusion of wave-current interaction, with results shown in Figures 11 and 12. For the case without coupling with ADCIRC, FVCOM, and SELFE, SWAN, SWAVE, and WWM showed that the significant wave height was high

Figure 14. Comparisons of the time series of significant wave height predicted by ADCIRC (red), FVCOM (blue), and SELFE (black) at sites A-F during 17–20 April 2007 for the cases without (left) and with (right) wave-current interaction.

over the shelf and low inside the harbor. After entering the harbor, the waves spread out toward both sides of the coast, resulting in relatively higher wave heights on the coast than in the interior. This spatial pattern remained unchanged for the case with wave-current interaction, except with an increase in significant wave height inside the harbor. For the case without wave-current interaction, the major differ-

ence was found near the coast along the inner shelf, where WWM-predicted significant wave height showed a larger cross-isobath gradient than SWAN and SWAVE. In addition, SWAN predicted a relatively higher significant wave height around the southwestern coast, which did not appear in SWAVE and WWM. For the case with inclusion of current-wave interaction, inside the harbor, FVCOM/

SWAVE showed a larger increase of the significant wave height on both northern and southern coasts, while ADCIRC/SWAN- and SELFE/WWM-predicted significant wave height distributions were more uniform. These differences were likely due to the discrete algorithms used to solve the wave models. SWAVE is solved using a second-order accurate upwind finite-volume scheme, whereas SWAN is solved using a first-order accurate finite-element scheme and WWM using a second-order Eulerian-Langragian finite-element scheme.

[37] The difference among the three models for wave prediction can be seen in more detail in the time series of the model-predicted significant wave height at sites A-F (Figures 13 and 14). For the case without wave-current interaction, SWAN- and SWAVE-predicted significant wave heights were very similar at sites A, B, D, and F for both the 2005 and 2007 events, while WWM-predicted significant wave heights were ~0.4 m higher than SWAN and SWAVE at site A, the same as SWAN and SWAVE at site B and site E, close to SWAVE at site C, and lower than SWAN and SWAVE at site D. For the case with wave-current interaction, all three models showed that the significant wave height increased dramatically and also varied with the M_2 tidal cycle at most stations. Significant differences in the significant wave height were found at sites A, C, and D. ADCIRC/SWAN and FVCOM/SWAVE, for example, consistently showed a large variation of significant wave height at site D, while the SELFE/WWM-predicted significant wave height was very low and did not change much with time. These differences remained the same for both the 2005 and 2007 events.

[38] The significant differences found in the wave simulations in these three wave models help explain why the model-predicted coastal inundation and water flux differed in both space and time among ADCIRC/SWAN, FVCOM/SWAVE, and SELFE/WWM for the case with wave-current interaction.

5. Summary

[39] ADCIRC/SWAN, FVCOM/SWAVE, and SELFE/WWM were evaluated for simulating extratropical storm-induced coastal inundation in Scituate Harbor, MA, for the late May 2005 and April 2007 Patriot's Day nor'easters. For the same unstructured grid, meteorological forcing, and initial/boundary conditions, intermodel comparisons were made for tidal elevation, surface waves, sea surface elevation, coastal inundation, currents, and volume transport.

[40] All three models showed similar accuracy in tidal simulation and consistent dynamic responses to storm winds in experiments conducted without and with wave-current interaction. The three models also showed that wave-current interaction could (1) change the current direction from the along-shelf direction to the onshore direction over the northern shelf, enlarging the onshore water transport and (2) intensify an anticyclonic separation eddy in the harbor entrance and a cyclonic eddy in the harbor interior, leading to an increased water transport into the harbor toward the northern peninsula and the southern end and thus enhance flooding in those areas. The testbed intermodel comparisons suggest that major differences in the performance of the three models occurred for the case with the inclusion of wave-current interaction. Under the same forcing condition, the differences found in the wave simulations in SWAN, SWAVE, and WWM explain to a certain degree why the model-predicted coastal inundation and water flux differed in both space and time among these three models. The differences were also related to the different discrete algorithms used to solve the three wave models, compute water-current interaction, use different wet-dry point treatments to simulate inundation, and different bottom friction parameterizations.

[41] It should be pointed out here that the intermodel comparison described here was made with a focus on dynamic responses of the models to storm-induced winds and boundary forcing. Since there was the lack of direct measurements of water elevation, significant wave height, and inundation areas, the results could not be used to evaluate the numerical accuracy of these models. Since the WFO tide gauge was established inside Scituate Harbor in December 2008, there was a full record of water elevation measurements made during the 27 December 2010 nor'easter. With the same grid configuration, Beardsley et al. (Coastal flooding in Scituate (MA): A FVCOM study of the Dec. 27, 2010 nor'easter, submitted to *Journal of Geophysical Research: Oceans*, 2013) applied the Scituate FVCOM inundation model to simulate the storm-induced surge level and flooded area, which agreed reasonably well with observations.

References

Abgrall, R. (2006), Residual distribution schemes: Current status and future trends, *Comput. Fluids*, *35*(7), 641–669, doi:10.1016/j.compfluid. 2005.01.007.

Bernier, N., and K. R. Thompson (2006), Predicting the frequency of storm surges and extreme sea levels in the northwest Atlantic, *J. Geophys. Res.*, *111*, C10009, doi:10.1029/2005JC003168.

Bertin, X., A. Oliveira, and A. B. Fortunato (2009), Simulating morphodynamics with unstructured grids: Description and validation of a modeling system for coastal applications, *Ocean Modell.*, *28*(1–3), 75–87.

Brovchenko, I., V. Maderich, and K. Terletska (2011), Numerical simulations of 3D structure of currents in the region of deep canyons on the east coast of the Black Sea, *Int. J. Comput. Civil Struct. Eng.*, *7*(2), 47–53.

Bunya, S., et al. (2010), A high resolution coupled riverine flow tide, wind, wind wave and storm surge model for southern Louisiana and Mississippi: Part I—Model development and validation, *Mon. Weather Rev.*, *138*, 345–377.

Burchard, H. (2002), *Applied Turbulence Modeling in Marine Waters*, 215 pp., Springer, Berlin.

Burla, M., A. M. Baptista, Y. Zhang, and S. Frolov (2010), Seasonal and interannual variability of the Columbia River plume: A perspective enabled by multiyear simulation databases, *J. Geophys. Res.*, *115*, C00B16, doi:10.1029/2008JC004964.

Chen, C., H. Liu, and R. Beardsley (2003), An unstructured grid, finite-volume, three dimensional, primitive equations ocean model: Application to coastal ocean and estuaries, *J. Atmos. Oceanic Technol.*, *20*(1), 159–186.

Chen, C., R. C. Beardsley, and G. Cowles (2006a), An unstructured grid, finite-volume coastal ocean model (FVCOM) system, Special issue titled "Advances in Computational Oceanography," *Oceanography*, *19*(1), 78–89.

Chen, C., G. Cowles, and R. C. Beardsley (2006b), An Unstructured-Grid, Finite-Volume Coastal Ocean Model: FVCOM User Manual, 2nd ed., School for Marine Science and Technology, *SMAST/UMASSD Tech. Rep. 06-0602*, pp. 315, University of Massachusetts-Dartmouth, New Bedford, MA.

Chen, C., H. Huang, R. C. Beardsley, H. Liu, Q. Xu, and G. Cowles (2007), A finite-volume numerical approach for coastal ocean circulation studies: Comparisons with finite difference models, *J. Geophys. Res.*, *112*, C03018, doi:10.1029/2006JC003485.

Chen, C., J. Qi, C. Li, R. C. Beardsley, H. Lin, R. Walker, and K. Gates (2008), Complexity of the flooding/drying process in an estuarine tidal-creek salt-marsh system: An application of FVCOM, *J. Geophys. Res.*, *113*, C07052, doi:10.1029/2007JC004328.

Chen, C., G. Gao, J. Qi, A. Proshutinsky, R. C. Beardsley, Z. Kowalik, H. Lin, and G. Cowles (2009), A new high-resolution unstructured-grid finite-volume Arctic Ocean model (AO-FVCOM): An application for tidal studies, *J. Geophys. Res.*, *114*, C08017, doi:10.1029/2008JC004941.

Chen, C., et al. (2011), An Unstructured-Grid, Finite-Volume Community Ocean Model FVCOM User Manual, 3rd ed., *SMAST/UMASSD Tech. Rep. 11–1101*.

Craig, P. D., and M. L. Banner (1994), Modeling wave-enhanced turbulence in the ocean surface layer, *J. Phys. Oceanogr.*, *24*(12), 2546–2559.

Dawson, C., J. J. Westerink, J. C. Feyen, and D. Pothina (2006), Continuous, discontinuous and coupled discontinuous-continuous Galerkin finite element methods for the shallow water equations, *Int. J. Numer. Methods Fluids*, *52*, 63–88.

Dietrich, J. C., et al. (2010), A high resolution coupled riverine flow, tide, wind, wind wave and storm surge model for southern Louisiana and Mississippi: Part II—Synoptic description and analyses of hurricanes Katrina and Rita, *Mon. Weather Rev.*, *138*, 378–404.

Dietrich, J. C., et al. (2011), Hurricane Gustav (2008) waves and storm surge: Hindcast, synoptic analysis and validation in southern Louisiana, *Mon. Weather Rev.*, *139*, 2488–2522, doi:10.1175/2011MWR3611.1.

Dietrich, J. C., et al. (2012), Performance of the unstructured-mesh, SWAN + ADCIRC model in computing hurricane waves and surge, *J. Sci. Comput.*, *52*, 468–497, doi:10.1007/s10915-011-9555-6.

Donelan, A. M., F. W. Dobson, S. D. Smith, and R. J. Anderson (1993), On the dependence of sea surface roughness on wave development, *J. Phys. Oceanogr.*, *23*, 2143–2149.

Dudhia, J., D. Gill, K. Manning, W. Wang, C. Bruyere, J. Wilson, and S. Kelly (2003), PSU/NCAR mesoscale modeling system tutorial calss notes and user's guide. MM5 modeling system version 3, Mesoscale and Mircroscale Meteorology Division, National Center for Atmospheric Research, 390pp.

FEMA (2009), *Flood insurance study: Southeastern Parishes*, Louisiana: Offshore water levels and waves, U.S. Army Corps of Eng., New Orleans, La.

Gao, G., C. Chen, J. Qi, and R. C. Beardsley (2011), An unstructured-grid, finite-volume sea ice model: Development, validation, and application, *J. Geophys. Res.*, *116*, C00D04, doi:10.1029/2010JC006688.

Grant, W. D., and O. S. Madsen (1979), Combined wave and current interaction with a rough bottom, *J. Geophys. Res.*, *84*(C4), 1797–1808.

Hope, M. E., et al. (2013), Hindcast and validation of hurricane Ike (2008), waves, forerunner, and storm Surge, *J. Geophys. Res.*, doi:10.1029/2013JC008879, in press.

Huang, H., C. Chen, G. W. Cowles, C. D. Winant, R. C. Beardsley, K. S. Hedstrom, and D. B. Haidvogel (2008), FVCOM validation experiments: Comparisons with ROMS for three idealized barotropic test problems, *J. Geophys. Res.*, *113*, C07042, doi:10.1029/2007JC004557.

Kennedy, A. B., et al. (2011), Origin of the Hurricane Ike forerunner surge, *Geophys. Res. Lett.*, *38*, L08608, doi:10.1029/2011GL047090.

Komen, G. J., L. Cavaleri, M. Donelan, K. Hasselmann, S. Hasselmann, and P. A. E. M. Janssen (1996), *Dynamics and Modelling of Ocean Waves*, p. 532, Cambridge Univ. Press, Cambridge, United Kingdom.

Lai, Z., C. Chen, G. Cowles, and R. C. Beardsley (2010a), A non-hydrostatic version of FVCOM, Part I: Validation experiments, *J. Geophys. Res.*, *115*, C11010, doi:10.1029/2009JC005525.

Lai, Z., C. Chen, G. Cowles, and R. C. Beardsley (2010b), A non-hydrostatic version of FVCOM, Part II: Mechanistic study of tidally generated nonlinear internal waves in Massachusetts Bay, *J. Geophys. Res.*, *115*, C12049, doi:10.1029/2010JC006331.

Longuet-Higgins, M. S., and R. W. Stewart (1964), Radiation stresses in water waves; a physical discussion, with applications, *Deep Sea Res. Oceanogr. Abstr.*, *11*(4), 529–562.

Luettich, R. A., and J. J. Westerink (2004), Formulation and numerical implementation of the 2D/3D ADCIRC finite element model version 44.XX. [Available at http://adcirc.org/adcirc_theory_2004_12_08.pdf.]

McFadden, R. (2007), East Coast Storm breaks rainfall records, New York Times, 17 April.

Mellor, G. L., and T. Yamada (1982), Development of a turbulence closure model for geophysical fluid problem, *Rev. Geophys. Space. Phys.*, *20*, 851–875.

National Weather Center (NWC) (2007), Spring 2007 Nor'easter, NOAA, University of Oklahoma, Norman, Okla.

Pawlowicz, R., B. Beardsley, and S. Lentz (2002), Classical tidal harmonic analysis with error analysis in MATLAB using T_TIDE, *Comput. Geosci.*, *28*, 929–937.

Qi, J., C. Chen, R. C. Beardsley, W. Perrie, Z. Lai, and G. Cowles (2009), An unstructured-grid finite-volume surface wave model (FVCOM-SWAVE): Implementation, validations and applications, *Ocean Modell.*, *28*, 153–166, doi:10.1016/j.ocemod. 2009.01.007.

Roland, A. (2009), Development of WWM II: Spectral wave modeling on unstructured meshes, PhD dissertation, Tech. Univ. Darmstadt, Inst. of Hydraul. and Water Resour. Eng, Darmstadt, Germany.

Signell, R. P., and J. H. List (1997), Effect of wave enhanced bottom friction on storm-driven circulation in Massachusetts Bay, *J. Waterway, Port, Coastal, Ocean Eng.*, *123*(5), 233–239.

Skamarock, W. C., and J. B. Klemp (2008), A time-split nonhydrostatic atmospheric model for research and NWP applications, Special issue on Environmental Modeling, *J. Comp. Phys.*, *227*, 3465–3485, doi:10.1016/j.jcp.2007.01.037.

Smagorinsky, J. (1963), General circulation experiments with the primitive equations, I. The basic experiment, *Mon. Weather Rev.*, *91*, 99–164.

Tolman, H. L. (1992), Effects of numerics on the physics in a third generation wind-wave model, *J. Phys. Oceanogr.*, *22*(10), 1095–1111.

Tanaka, S., S. Bunya, J. J. Westerink, C. Dawson, and R. A. Luettich (2011), Scalability of an unstructured grid continuous Galerkin based hurricane storm surge model, *J. Sci. Comput.*, *46*, 329–358.

USACE (2009), Hydraulics and hydrology appendix, Louisiana coastal protection and restoration: Final technical report, p. 389, U.S. Army Engineer, New Orleans, La.

Warner, J. C., C. R. Sherwood, R. P. Signell, C.K. Harris, and H. G. Arango (2008), Development of a three-dimensional, regional, coupled wave, current, and sediment-transport model, *Computers and Geosciences*, *34*(10), 1284–1306, doi:10.1016/j.cageo.2008.02.012.

Wu, L., C. Chen, F. Guo, M. Shi, J. Qi, and J. Ge (2010), A FVCOM-based unstructured grid wave, current, and sediment transport model. I. Model description and validation, *J. Ocean. Univ. China*, *10*(1), 1–8, doi:10.1007/s11802-011-1788-3.

Zhang, Y., and A. M. Baptista (2008), SELFE: A semi-implicit Eulerian–Lagrangian finite-element model for cross-scale ocean circulation, *Ocean Modell.*, *21*(3–4), 71–96.

Zhang, Y., R. C. Witter, and G. R. Priest (2011), Tsunami-tide interaction in 1964 Prince William Sound tsunami, *Ocean Modell.*, *40*(3–4), 246–259.

Zijlema, M. (2010), Computation of wind-wave spectra in coastal waters with SWAN on unstructured Grids, *Coastal Eng.*, *57*, 267–277.